ISTANBUL TECHNICAL UNIVERSITY ★ GRADUATE SCHOOL

JIG SHAPE OPTIMIZATION FOR DESIRED SHAPE OF A HIGH-ALTITUDE LONG-ENDURANCE CLASS UNMANNED AERIAL VEHICLE UNDER AEROELASTIC EFFECTS

M.Sc. THESIS

Akın ATEŞ

Department of Computational Science and Engineering

Computational Science and Engineering Programme

JULY 2024

ISTANBUL TECHNICAL UNIVERSITY ★ GRADUATE SCHOOL

JIG SHAPE OPTIMIZATION FOR DESIRED SHAPE OF A HIGH-ALTITUDE LONG-ENDURANCE CLASS UNMANNED AERIAL VEHICLE UNDER AEROELASTIC EFFECTS

M.Sc. THESIS

Akın ATEŞ
(702211001)

Department of Computational Science and Engineering

Computational Science and Engineering Programme

Thesis Advisor: Prof. Dr. Melike NİKBAY

JULY 2024

ISTANBUL TEKNİK ÜNİVERSİTESİ ★ LİSANSÜSTÜ EĞİTİM ENSTİTÜSÜ

HALE SINIFI BİR INSANSIZ HAVA ARACININ AEROELASTİK ETKİLER ALTINDA HEDEFLENEN ŞEKLE ULAŞMAK İÇİN JİG ŞEKLİ OPTİMİZASYONU

YÜKSEK LİSANS TEZİ

Akın ATEŞ
(702211001)

Hesaplamalı Bilim ve Mühendislik Ana Bilim Dalı

Hesaplamalı Bilim ve Mühendislik Programı

Tez Danışmanı: Prof. Dr. Melike NİKBAY

TEMMUZ 2024

Akın Ateş, a M.Sc. student of İTU Graduate School student ID 702211001 successfully defended the thesis entitled "JIG SHAPE OPTIMIZATION FOR DESIRED SHAPE OF A HIGH-ALTITUDE LONG-ENDURANCE CLASS UNMANNED AERIAL VEHICLE UNDER AEROELASTIC EFFECTS", which he prepared after fulfilling the requirements specified in the associated legislations, before the jury whose signatures are below.

Thesis Advisor :	**Prof. Dr. Melike NİKBAY** İstanbul Technical University	.....
Jury Members :	**Prof. Dr. Fırat Oğuz EDİS** İstanbul Technical University	.....
	Dr. Serhat YILMAZ National Defence University	.....

Date of Submission : 24 May 2024
Date of Defense : 24 July 2024

To my family,

FOREWORD

First, I extend my sincere gratitude to Prof. Dr. Melike Nikbay, for her invaluable guidance and contributions to this work. Prof. Dr. Melike Nikbay's insightful advice, wealth of experience, and supportive approach have played a crucial role in shaping this study. Therefore, I am deeply thankful to Prof. Dr. Melike Nikbay and express my utmost gratitude to her.

Additionally, I would like to express my gratitude to Turkish Aerospace Industries for providing the resources used in this study. The company's advancements, expertise, and innovations have greatly influenced and inspired this research, significantly contributing to the growth and development of aerospace engineering in Turkey.

July 2024 Akın ATEŞ

TABLE OF CONTENTS

Page

ABBREVIATIONS

AIC : Aerodynamic Influence Coefficient
AOA : Angle of Attack
CAD : Computer-Aided Design
CFD : Computational Fluid Dynamics
FEM : Finite Element Method
PDR : Preliminary Design Review
SQP : Sequential Quadratic Programming
SLP : Sequential Linear Programming
UAV : Unmanned Aerial Vehicle
HALE : High-Altitude Long-Endurance
RANS : Reynolds-Averaged Navier-Stokes

SYMBOLS

$\mathbf{M}_\infty$	: Freestream Mach Number
$\boldsymbol{\varphi}$	: Perturbation Potential
$\boldsymbol{\tau}$	: Thickness Ratio
u,v	: Displacement Vector Components
[K]	: Stiffness Matrix
$[\boldsymbol{G}]^{\boldsymbol{T}}$	: Spline Matrix
$[\boldsymbol{AIC}]$	: Aerodynamic Influence Coefficient Matrix
$\{\boldsymbol{X}\}$	: Structural deformation
$\boldsymbol{F_R}$	: Mapped Rigid Loads
$[\boldsymbol{M}]$	: Mass Matrix
$\{\ddot{\boldsymbol{u}}\}$	: Aircraft Rigid Body Accelerations
$[\boldsymbol{K_{ee}}]$	: Generalized Stiffness Matrix of the Elastic Modes
$[\boldsymbol{Q}]$	: Generalized Aerodynamic Force Matrix
$\boldsymbol{S_{kj}}$	: Integration Matrix to Convert Pressure to Forces
$\boldsymbol{q}_\infty$	: Dynamic Pressure
$\boldsymbol{x_0}$	: Initial Guess of Optimization
$\boldsymbol{v_i^x}$	: *X* Coordinates of Nodes
$\boldsymbol{v_i^y}$	: *Y* Coordinates of Nodes
$\boldsymbol{v_i^z}$	: *Z* Coordinates of Nodes
N(i)	: Neighbors of the Node
$\boldsymbol{\theta}$	: Twist Angle
Γ	: Section Displacement
C	: Chord Length
S	: Wing Area
b	: Wing Span
St	: Station

LIST OF TABLES

Page

LIST OF FIGURES

Page

JIG SHAPE OPTIMIZATION FOR DESIRED SHAPE OF A HIGH-ALTITUDE LONG-ENDURANCE CLASS UNMANNED AERIAL VEHICLE UNDER AEROELASTIC EFFECTS

SUMMARY

The field of aviation is continuously developing, and with advancements in technology, it has established a strong foundation. The desire to integrate air travel into everyday life has accelerated the design and production processes of aircraft. In civil aviation, aircraft are designed with the aim of reducing fuel costs, flying over long distances, and carrying the maximum number of passengers. The military sector, on the other hand, emphasizes features such as flying faster, reaching higher altitudes, and carrying weapons and missiles. Meeting these diverse requirements is possible through the most efficient design of power systems, structures, and aerodynamics in the aircraft. Since engine design falls outside the scope of this thesis, this thesis focuses on aerodynamic and structural design.

The desire to make aircraft lighter to achieve better performance has increased. With the advancement in material technology, stronger and lighter aerospace materials have been developed. These lightweight materials are more flexible compared to traditional materials, making them ideal for modern day designs. While aircraft produced with these materials are 30% lighter than those produced with conventional materials, they are also more susceptible to elastic effects. Therefore, to fully realize the benefits of weight reduction, it is crucial to examine the aeroelastic effects on the aircraft in more detail.

The field of aeroelasticity focuses on understanding and addressing the combined effects of inertial, elastic, and aerodynamic forces. Its popularity, within the aircraft design community, is constantly increasing as aircraft are becoming more and more flexible. Aeroelasticity is generally divided into two main categories: static aeroelasticity and dynamic aeroelasticity. Some of the common phenomena associated with static aeroelasticity include control reversal, effectiveness, and divergence, while the phenomena associated with dynamic aeroelasticity include buzz, buffet, gust, and flutter. In the aircraft design process, once the conceptual design is finalized during the preliminary design stage, the aerodynamicists start to work on the external geometry to achieve an optimal design. This aerodynamically optimized wing is then handed over to structural engineers, who manufacture it within specified production tolerances. These manufacturing constraints cause the aircraft's external surface to deviate slightly from its optimized design. In summary, there are geometrical differences between the optimal aerodynamic design and the manufactured geometry. These differences result in discrepancies between the calculated performance values of the optimized design and the actual performance values of the manufactured geometry.

When the the loss due to geometrical difference is added the aerodynamic performance values will significantly decrease. The external geometry of an aircraft is a dynamic, living cycle. It undergoes many changes from design to production. These external shapes are generally divided into two groups: theoretical shapes and practical shapes. Examples of theoretical shapes include the 1G flight shape, jig shape, and engineering shape. Examples of practical shapes include the manufacturing shape, parking shape, actual flight shape, and operation shape.

The aim of this study is to arrive at a more effective design during the preliminary design stage of the aircraft design process by incorporating a multidisciplinary approach. Due to time constraints in aircraft design processes, designers often avoid complex and expensive analyses. This study proposes a method to mitigate these challenges by providing a quick solution for integrating multidisciplinary analysis into the preliminary design stage, thereby enabling a more effective design process.

In this study, the RQ-4 Global Hawk, a HALE class unmanned aerial vehicle, is selected. The reason for choosing the RQ-4 Global Hawk is that it has very large aspect ratio making the elastic effects more apparent. Initially, the point cloud data available in the literature for the RQ-4 Global Hawk is acquired. A structured mesh capable of creating this point cloud is generated using a Python coded. This mesh is employed to establish a ZONAIR aerodynamic model, a 3D panel method that uses high-order panels. The results obtained using the ZONAIR aerodynamic model was validated against the available flight data in literature.

The same grid are used for the structural analysis of the RQ-4 Global Hawk. The material density is chosen based on the real-life weight of the RQ-4 Global Hawk. The weight distribution is made proportional to the volumes of the RQ-4 Global Hawk's components. The FEM analysis of the RQ-4 Global Hawk is performed with composite materials, using stiffness values found in the literature. A modal analysis is then conducted to determine the natural modes and frequencies related to the wing.

After preparing the ZONAIR aerodynamic model and FEM model of the RQ-4 Global Hawk aircraft, the ZONAIR model is made ready for aero-structural coupling. For specific Mach numbers and angles of attack, both the rigid (desired) and elastic (flight shape) results are obtained.

Since the RQ-4 Global Hawk is a subsonic aircraft, the chosen angles of attack and Mach numbers show linear values in the graphs. This is advantageous for UAV because improving one design point aeroelastically will automatically improve other design points as well. In light of this information, the differences in lift coefficients between the flight shape and the rigid shape are measured. The results indicate a 5.5% aerodynamic loss between the flight shape and the rigid shape. This difference is a significant loss for aircraft.

This difference arises due to the elastic structure of the RQ-4 Global Hawk. To minimize the loss caused by elastic effects, a solution method is developed in this thesis. Defining and applying the jig shape in the design process is crucial to prevent the loss caıse by elastic effects. There are two ways to address the difference caused by elastic effects: the first is structural reinforcement, which is generally undesirable. As increasing stiffness automatically increases weight. In this study, the other method, managing deflections and twists, is exemined.

The importance of jig shape design has increased in the aircraft design process. In this study, the main goal is to incorporate jig shape design into the preliminary design process and develop a methodology. A methodology for rigid, elastic, and jig shape design is developed and used iteratively for design optimization.

Generally speaking, the procedure involves taking an aerodynamically optimized wing as the target shape. Next, rigid and elastic solutions are obtained at specific design points for this target shape. In the elastic solution, the loads are extracted. These extracted, inverted and applied to the aircraft to obtain an aero-structural solution and identify the initial jig shape. The initial jig shape of the aircraft is found. This initial

jig shape is then subjected to the same conditions in an aero-structural solution, and the new flight shape is measured. In the next step, the new flight shape is compared to the target shape. If the difference between the new flight shape and the target shape is below a certain limit, the iteration ends. If it is exceeds the limit, the process starts over. The loads from the new flight shape are inverted, and the jig shape for the second iteration is found. This is then subjected to the ZONAIR aero-structural solution to obtain the flight shape, which is compared again to the target shape.

The methodology developed in this study is both fast and practical, requiring many iterations are needed to find the most optimal jig shape. Optimization methods have been used to make this process more intelligent. Especially, a stable and widely used optimization method has been selected. The aim of this study is to simplify complex models to achieve faster solutions, so a fast-working gradient-based optimization method, SQP, has been chosen as the optimization method. A effective optimization model has also been established for the RQ-4 Global Hawk aircraft, automating the jig shape optimization procedure. This procedure enhances the aircraft design process by enabling raid jig shape optimization during the preliminary design stage. This jig shape optimization increases the efficiency of the aircraft, making it more effective. Jig shape optimization is a process that contributing to reaching the targeted range and achieving more successful observations and weapon firings in the field.

HALE SINIFI BİR INSANSIZ HAVA ARACININ AEROELASTİK ETKİLER ALTINDA HEDEFLENEN ŞEKLE ULAŞMAK İÇİN JİG ŞEKLİ OPTİMİZASYONU

ÖZET

Havacılık alanı sürekli olarak gelişiyor ve teknolojinin ilerlemesiyle sağlam bir temel oluşturmuştur. Hava araçlarını günlük yaşama entegre etme isteği, hava aracı tasarım ve üretim süreçlerini hızlandırmıştır. Sivil havacılıkta, hava araçları yakıt maliyetlerini azaltma, uzun mesafelere uçma ve maksimum yolcu taşıma amacıyla tasarlanır ve üretilir, çünkü bunlar kâr amacı güden işletmelerdir. Askeri alanda ise daha hızlı uçma, yüksek irtifalara çıkma ve silah ve füzeler taşıma gibi özellikler önemlidir. Bu gereksinimlerin karşılanması, hava aracının güç sistemleri, yapıları ve aerodinamiğinin en verimli şekilde tasarlanmasıyla mümkündür. Motor tasarımı bu tezin kapsamı dışında olduğu için, tez aerodinamik ve yapısal tasarıma odaklanmaktadır.

Hava araçlarını daha hafif yaparak daha yüksek performans elde etme isteği artmıştır. Malzeme teknolojisinin ilerlemesiyle, daha güçlü ve daha hafif havacılık malzemeleri geliştirilmiştir. Bu malzemeler, çok hafif oldukları için geleneksel malzemelere göre daha esnek yapıya sahiptirler. Bu malzemelerle üretilen hava araçları, geleneksel malzemelerle üretilenlere göre %30 daha hafif olmaktadır. Doğal olarak, daha hafif bir hava aracı daha yüksek performansa sahip olacaktır; ancak, elastik etkiler performansını etkileyecektir. Bu hafiflemenin bir bedeli olarak, hava aracındaki aeroelastik etkiler daha detaylı bir şekilde incelenmelidir.

Aeroelasticity alanı, atalet, elastik ve aerodinamik kuvvetlerin bir arada çözülmesini amaçlar. Hava araçları daha esnek hale geldikçe bu alanın popülaritesi artmakta ve hava aracı tasarım topluluğunun ilgisini çekmektedir. Aeroelasticity genellikle statik aeroelasticity ve dinamik aeroelasticity olmak üzere iki ana kategoriye ayrılır. Statik aeroelasticity örnekleri arasında kontrol ters dönüşü, etkililik ve ayrışma yer alırken; dinamik aeroelasticity örnekleri arasında buzz, buffet, gust ve flutter yer alır. Hava aracı tasarım sürecinde, ön tasarım aşamasında konsept tasarım belirlendikten sonra, tasarım süreci aerodinamikçilerin dış geometri tasarımı üzerinde çalışmalarıyla başlar. Aerodinamik açıdan optimize edilmiş bir kanat tasarlanır. Bu aerodinamik açıdan optimize edilmiş kanat, daha sonra yapısal mühendislere teslim edilerek belirli üretim toleranslarıyla üretilir. Bu üretim toleransları, hava aracının dış yüzeyinin optimize edilmiş tasarımdan biraz sapmasına neden olur. Özetlemek gerekirse, aerodinamik açıdan mükemmel şekilde optimize edilmiş geometri ile üretilen geometri arasında farklar vardır. Bu farklar, hesaplanan performans değerleri ile üretilen geometrinin gerçek performans değerleri arasında uyumsuzluklara neden olur.

Elastik etkilerden kaynaklanan kayıp bu farka eklenirse, aerodinamik performans değerleri önemli ölçüde azalacaktır. Bir hava aracının dış geometrisi dinamik, yaşayan bir döngüdür. Tasarımdan üretime kadar birçok değişiklik geçirir. Bu dış şekiller genellikle iki gruba ayrılır: teorik şekiller ve pratik şekiller. Teorik şekillere örnek olarak 1G uçuş şekli, jig şekli ve mühendislik şekli verilebilir. Pratik şekillere örnek olarak ise imalat şekli, park etme şekli, gerçek uçuş şekli ve operasyon şekli verilebilir.

Bu çalışmanın amacı, hava aracı tasarım sürecinin ön tasarım aşamasında çok disiplinli bir yaklaşımı dahil ederek daha etkili bir tasarım yapmaktır. Hava aracı tasarım süreçlerinde zaman baskısı olduğundan, tasarımcılar genellikle zor ve maliyetli analizlerden kaçınırlar. Bu çalışma, çok disiplinli analizi ön tasarım aşamasına hızlı bir şekilde dahil edebilecek bir yöntem önermektedir. Bu çalışmada, HALE sınıfı bir insansız hava aracı olan RQ-4 Global Hawk seçilmiştir. RQ-4 Global Hawk'ın seçilme nedeni, çok büyük aspect ratio değerine sahip olmasıdır, bu da elastik etkileri daha belirgin hale getirir. Bu nedenle RQ-4 Global Hawk tercih edilmiştir. İlk olarak, literatürde bulunan RQ-4 Global Hawk için mevcut nokta bulutu verisi alınmıştır. Python dilinde yazılmış bir kod kullanılarak bu nokta bulutunu oluşturabilen yapılandırılmış bir ağ oluşturulmuştur. RQ-4 Global Hawk'ın yapılandırılmış ağıyla, ZONAIR aerodinamik modeli kurulmuştur. ZONAIR, yüksek düzeyde bir panel tekniği kullanarak 3 boyutlu bir panel yöntemidir. RQ-4 Global Hawk için ZONAIR aerodinamik modeli kurulduktan sonra, RQ-4 Global Hawk'ın uçuş verileri kullanılarak doğrulanmıştır. RQ-4 Global Hawk, başarılı bir aerodinamik model olarak kanıtlanmıştır.

Aynı mesh noktaları, RQ-4 Global Hawk'ın yapısal modeli için de kullanılmıştır. Malzeme yoğunluğu, RQ-4 Global Hawk'ın gerçek hayattaki ağırlığına göre girilmiştir. Ağırlık dağılımı, RQ-4 Global Hawk'ın bileşenlerinin hacimlerine orantılı olarak yapılmıştır. RQ-4 Global Hawk'ın FEM modeli kompozit malzemelerle modellenmiş ve literatürde bulunan sertlik değerleri kullanılarak oluşturulmuştur. RQ-4 Global Hawk'ın FEM modelinin modal analizi yapılmış ve kanat ile ilgili doğal modlar ve frekanslar belirlenmiştir.

RQ-4 Global Hawk hava aracının ZONAIR aerodinamik modeli ve FEM modeli hazırlandıktan sonra ZONAIR modeli aero-yapısal bağlantı için hazır hale getirilir. Belirli Mach numaraları ve saldırı açıları için RQ-4 Global Hawk'ın hem rijit (istenen) hem de elastik (uçuş şekli) sonuçları elde edilir.

RQ-4 Global Hawk'ın bir subsonik uçak olması nedeniyle seçilen hücum açıları ve Mach numaraları grafiklerde lineer değerler gösterir. Bu durum, bir tasarım noktasını aeroelastik olarak iyileştirmenin diğer tasarım noktalarını da otomatik olarak iyileştirmesinin avantajlı olduğunu gösterir. Bu bilgiye göre, uçuş şekli ile rijit şekil arasındaki kaldırma kuvveti farkları ölçülür. Sonuçlar, uçuş şekli ile rijit şekil arasında %5.5'lik bir aerodinamik kayıp olduğunu göstermektedir. Bu fark, uçaklar için önemli bir kayıptır.

Bu fark, RQ-4 Global Hawk'ın elastik yapısından kaynaklanır. Elastik etkilerden kaynaklanan kaybı en aza indirmek için bu tezde bir çözüm yöntemi geliştirilmiştir. Elastik etkilerden kaynaklanan kaybı önlemek için tasarım sürecinde jig şeklinin tanımlanması ve uygulanması hayati öneme sahiptir. Elastik etkilerden kaynaklanan farkı ele almanın iki yolu vardır: birincisi genellikle istenmeyen yapısal güçlendirme yöntemidir. Sertliği artırmak otomatik olarak ağırlığı artırır. Bu çalışmada, diğer yöntem olan deformasyonları ve dönüşleri yönetme tercih edilir.

Hava aracı tasarım sürecinde jig şekil tasarımının önemi artmıştır. Bu çalışmada, jig şekil tasarımını ön tasarım sürecine dahil etmek ve bir metodoloji geliştirmek amaçlanmaktadır. Rijit, elastik ve jig şekil tasarımı için bir metodoloji geliştirilmiş ve tasarım optimizasyonu için tekrarlı olarak kullanılmıştır.

Genel olarak, prosedür aerodinamik olarak optimize edilmiş bir kanadın hedef şekil olarak alınmasını içerir. Bu hedef şekil için, belirli tasarım noktalarında sert ve elastik çözümler elde edilir. Elastik çözümde yükler çıkarılır. Çıkarılan bu yükler ters çevrilir ve hava aracına uygulanır ve bir aero-yapısal çözüm elde edilir. Hava aracının başlangıç jig şekli bulunur. Bu başlangıç jig şekli daha sonra bir aero-yapısal çözümde aynı koşullara tabi tutulur ve yeni uçuş şekli ölçülür. Bir sonraki adımda, yeni uçuş şekli hedef şekil ile karşılaştırılır. Eğer yeni uçuş şekli ile hedef şekil arasındaki fark belirli bir sınırdan düşükse, iterasyon sona erer. Eğer sınırdan yüksekse, süreç tekrar başlar. Yeni uçuş şekli yükleri ters çevrilir ve ikinci iterasyon için jig şekli bulunur. Bu daha sonra ZONAIR aero-yapısal çözüme tabi tutulur ve uçuş şekli elde edilir ve tekrar hedef şekil ile karşılaştırılır.

Bu çalışmada geliştirilen metodoloji hızlı ve pratiktir. Tabii ki, en optimal jig şeklini bulabilmek için birçok iterasyona ihtiyaç vardır. Bu süreci daha akıllıca hale getirmek için optimizasyon yöntemleri kullanılmıştır. Özellikle, stabil ve geniş bir şekilde kullanılan bir optimizasyon yöntemi seçilmiştir. Bu çalışmanın amacı karmaşık modelleri basitleştirerek daha hızlı çözümler elde etmektir, bu nedenle hızlı çalışan gradyan tabanlı bir optimizasyon yöntemi olan SQP optimizasyon yöntemi olarak seçilmiştir. Ayrıca RQ-4 Global Hawk uçağı için başarılı bir optimizasyon modeli de kurulmuş, jig şekli optimizasyon prosedürü otomatize edilmiştir. Ön tasarım sürecinde hava aracı tasarımını daha etkili hale getirmek için çok kısa bir sürede jig şekli optimizasyonu yaparak bir prosedür geliştirilmiştir. Bu jig şekli optimizasyonu, hava aracının verimliliğini artırarak daha etkili hale getirir. Jig şekli optimizasyonu, hedeflenen menzile ulaşmaya ve sahada daha başarılı gözlemler ve silah atışları gerçekleştirmeye katkı sağlayan bir süreçtir.

1. INTRODUCTION

Unmanned Aerial Vehicles (UAVs) play a pivotal role in modern aviation. They offer extended flight capabilities for missions such as surveillance, reconnaissance, communication, and environmental monitoring. High-Altitude Long-Endurance (HALE) UAVs represent a distinct class of UAVs designed for missions requiring prolonged flight times at high altitudes. These vehicles typically employ high aspect ratio wings and hence their performance is significantly impacted by the aerodynamic loads and aeroelastic effects. Aeroelasticity, the interaction between inertial, elastic, and aerodynamic forces, can cause geometric deformations that alter a UAV's aerodynamic characteristics, impacting its efficiency and control.

To achieve the best performance and stability, the aerodynamic shape of a HALE class UAV must be carefully designed and maintained during flight, even when affected by aeroelastic effects. A deeper understanding on how these effects occur during flight is necessary, to devise strategies for managing the deformations to protect the UAV's desired aerodynamic shape [1].

This thesis focuses on the critical aspect of optimizing the jig shape of a HALE class UAV to achieve and sustain its desired aerodynamic form under aeroelastic effects. By strategically managing deformations caused by aeroelastic forces, the goal is to prevent deviations from the desired aerodynamic shape and enhance overall aircraft performance. This process involves a comprehensive examination of the UAV's characteristics, the setup of aeroelastic models, evaluations of aeroelastic behaviors, and the optimization techniques utilized for jig shape design [2].

The following sections will delve into the specific methodologies employed, the results and discussions obtained, and the implications of optimizing jig shape for achieving the desired aerodynamic performance. This comprehensive analysis aims to provide a clear understanding of how these optimizations contribute to enhancing overall flight efficiency. Additionally, the findings will highlight the potential benefits for future UAV design and development strategies.

1.1 Objective of Thesis

This thesis examines the optimization of jig shape to attain the desired aerodynamic form of a High-Altitude Long-Endurance (HALE) class unmanned aerial vehicle (UAV) under aeroelastic effects. The research aims to focus on managing deformations caused by aeroelastic effects during flight to prevent deviation from the desired aerodynamic shape. Aeroelastic effects can directly impact the performance of the UAV. Therefore, jig shape optimization plays a critical role in improving the UAV's targeted aerodynamic performance and ensuring resilience against aeroelastic effects during flight [3]. This thesis aims to make a significant contribution to improving UAV design by considering aeroelastic effects in optimizing jig shape.

1.2 Literature Survey

Aeroelasticity is a field that studies the interaction of aerodynamic, elastic, and inertial forces. This field is generally divided into two main categories: Static aeroelasticity and dynamic aeroelasticity. Static aeroelasticity examines the interaction of aerodynamic and elastic forces, including divergence and control reversal analyses. Dynamic aeroelasticity, on the other hand, investigates the interaction of aerodynamic, elastic, and inertial forces, covering analyses such as flutter, gust, and turbulence [5].

As aviation industry evolves, lighter and more flexible materials are being used to design high-performance aircraft. However, this increased flexibility can lead to significant deformation and twist in the wings[4]. Ultimately, despite aerodynamic optimization, the desired external aerodynamic surfaces can experience distortion due to twist and deformation, resulting in performance poor performance of the aircraft.

Elastic effects are crucial for both civilian and military aircraft. For instance, in civilian aviation, even a small aeroelastic improvement can lead to significant performance enhancements, resulting in substantial fuel saving. In the military domain, fighter jets like the F-22 and F-35 are meticulously designed to enable supercruise and transonic maneuvers, requiring the wings to stay within specific limits of twist and deformation to fulfill these two missions effectively [6]. Moreover, maintaining precise control over elastic deformation is essential to ensuring the aircraft's structural integrity and maneuverability under extreme flight conditions. This shows how important aeroelastic analysis is for designing and improving advanced aircraft systems.

In aircraft with a high aspect ratio wing, elastic effects are more pronounced, especially resulting in high deflection and twist values, which in turn leads to a decrease in aircraft stability and control [7]. Structural reinforcement can be used as a method, but this solution typically results in increased weight, thus acting as a penalty in aviation. Employing a smarter method to manage twist and deflection during flight, we can mitigate the performance loss due to elastic effects.

Unmanned aerial vehicles (UAVs) often prefer high aspect ratio wings to enhance glide efficiency, as these vehicles typically require extended endurance in the air for their missions [8]. High aspect ratio wings contribute to increased gliding capabilities. In the case of High-Altitude Long-Endurance (HALE) class aircraft, high aspect ratio wings are standard. Optimizing high aspect ratio wings goes beyond aerodynamic considerations as it also requires optimization from an aeroelastic perspective due to the significant elastic effects [9].

In aerodynamic design, aircraft wings are designed to achieve the best performance, which is referred to as the "desired shape. However, during flight, the shape that the aircraft takes is called the flight shape which is typically an aerodynamic shape under 1 G loading. Managing flight shape is crucial in aircraft design[10]. A concept called "jig shape" has been developed to reach the desired aerodynamic shape, and it is widely used in aviation [11]. Jig shape is an aircraft-level shape that is determined through an iterative process connected with calculating the flight shape [12].

Aeroelastic improvements, especially through jig shape optimization, will enable better management of flight shape, leading to more efficient operation of the aircraft's control surfaces. This is a desired feature in aircraft design [13]. Particularly in unmanned aerial vehicles (UAVs), efficient operation of control surfaces is sought because UAVs are expected to maintain stable flight. Jig shape optimization enhances aircraft controllability and flight dynamics.

Jig shape and jig shape optimization are becoming increasingly important in aviation day by day. These areas are of critical importance for enhancing aircraft aerodynamic performance, improving controllability, and optimizing flight dynamics. Especially in modern aviation technologies and unmanned aerial vehicle (UAV) design, the impact of jig shape optimization is growing [14]. These optimizations play a significant role in ensuring aircraft’s stability and control effectively. Literature review on jig shape

optimization, indicated that structural-weighted improvements and methods related to solution costs were commonly used. Zhang et al. argued that wing jig shape optimization requires significant computational resources for high-fidelity large-scale design problems [2]. Design problems, and gradient-based methods could be effective but may be limited in performance due to real-world issues like numerical noise and failed evaluations [2]. They introduced new developments in jig shape optimization using a gradient-assisted metamodel assembly technique within a trust-region optimization framework [2]. Their study demonstrated that the proposed method exhibits strong and efficient performance while keeping the additional time requirement for solutions under control. Ultimately, they established a loop between flight shape and jig shape for the UAV wing, optimizing the wing to achieve the desired shape [2].

Some studies have performed jig shape optimization using mesh regeneration methods for a high-aspect-ratio wing. In the mesh regeneration method, certain monitor stations were initially selected based on the structural characteristics of the wing. Subsequently, a new aerodynamic model was constructed based on the distribution of new monitor stations that maintain the same external points in each iteration. Finally, mesh generation and optimization quality control study was conducted [15]. Three different jig shape optimizations based on mesh regeneration is performed on a high-aspect-ratio wing. All of these jig shapes attempted to achieve designs that are suitable under the influence of static aeroelasticity. The lift coefficients of the three different jig shape optimizations were found to be larger than that of the original flat orginal wing. Considering both bending and torsion values, the results of the jig shape optimization are examined. Hue et al. Studied; original jig shape optimization, bending-only jig shape optimization, torsion-only optimization, and combined bending and torsion optimization. Lift coefficient results are analyzed for all cases, with the most efficient outcome achieved when both bending and torsion optimizations are performed [8].

NASA has shown interest in performance improvement studies for aircraft in terms of aerodynamics and aeroelasticity. Improvements have been made in other areas of aviation using jig shape optimization. Pak worked on the low-boom supersonic aircraft using jig shape optimization [6].

Bombardieri et al. used ONERA M6 and NASA CRM wings as test cases and performed aero-structural coupling solutions in SU2. The structural model was represented a stick model and the aerodynamic model in 3D. Euler and RANS equations were employed as the aerodynamic model. Gradient-based optimization methods selected. A gradient-based optimization was employed for successfully improving the aircraft performance [9]. However, this solution method is highly costly in terms of solving time and model setup.

Jig shape and related topics have become increasingly popular in recent years. Aircraft designers have started to take a deeper interest in the field of aeroelasticity, driven by advancements in optimization and multi-disciplinary areas. Sometimes, while solving an aeroelastic problem, one can inadvertently create new aeroelastic issues. For example, the weight addition solution under the wings to prevent flutter in subsonic aircraft. Such weight addition can disrupt the airflow under the wing, creating a vortex that interacts with the horizontal tail and potentially leading to the emergence of a buzz problem over time.

In the field of aeroelasticity, phenomena such as flutter, control reversal, buzz, and buffet have become popular, but the topic of jig shape, which is also part of aeroelasticity, has not gained much popularity. Advances in material technology, leading to the production of lighter wings, and increased knowledge in aerodynamic design have triggered the emergence of concepts like flight shape and jig shape, where aircraft outer mold lines vary. Aviation companies, especially those producing civilian aircraft, have experimented with various design improvement methods to design more efficient aircraft. One of their major challenges was the difference between the results obtained from computer-optimized wings and the actual flight data [11].

When examining studies related to jig shape, it was observed that expensive solutions were pursued. For instance, some studies involved performing jig shape calculations by coupling with Computational Fluid Dynamics (CFD) using RANS, which have long solution times. In some cases, the EULER equations were flow method was used, which is a bit faster than RANS, yet due to the complexity of structural and aerodynamic elements in the model, the overall time still remained extensive. In general, due to the complexity of aerodynamic and structural models, many studies have not totally converged [14].

Jig shape optimization is a long-term iterative analysis. Companies designing aircraft accept a certain amount of aerodynamic loss due to the known lengthy nature of this process, considering factors like time, labor, cost, and scheduling constraints. However, this study demonstrates how the aircraft's jig shape calculation and optimization can be done more quickly and practically using a different method.

This study aims to contribute to the design process by performing jig shape optimization using simpler panel methods that do not require complex and time-consuming models. Unlike most studies in the literature that use FSI tools, NASTRAN, and ZAERO, this study will utilize the ZONAIR tool. This study approach will significantly reduce the time required for jig shape calculation and optimization at the desired altitude and speed, providing a valuable contribution to the literature [20].

Studies related to jig shape often propose long and laborious solutions that involve changing internal structural layouts, similar to structural optimization. However, the present approach optimizes only the external surface (outer mold lines) within certain limits without altering the internal structural layout, including ribs, spars, and their locations. This approach will play a significant role in enhancing the aerodynamic efficiency of aircraft design. Although we typically design the wing based on desired aerodynamic and aeroelastic conditions, in reality, we may deviate from the intended flight shape. It is important to calculate this deviation more quickly and use this information to improve aircraft design, making this study crucial.

1.3 Hypothesis

The hypothesis of this study is that jig shape optimization will contribute to improving the aerodynamic efficiency of aircraft, enabling them to reach the intended range and produce high-performance aircraft, thus contributing to more successful observations and weapon firings in the field.

2. MODEL DEFINITION

UAV is selected for this study because of their high aspect ratio wings, which provide a clearer view of aeroelastic effects. Their combination of high aspect ratio wings and prominent elastic effects makes UAVs ideal for studying aerodynamic performance and understanding aeroelastic effects. High aspect ratio wings are particularly crucial for extended flights. A detailed analysis of aerodynamic modifications and aeroelastic effects on high aspect ratio wings is essential for attaining the desired aerodynamic profile.

2.1 Configuration Selection

In this study, an unmanned aerial vehicle of HALE (High-Altitude Long-Endurance) class with a high aspect ratio wing, namely the RQ-4 Global Hawk aircraft, has been selected. The RQ-4 Global Hawk is a high-altitude long-range unmanned aerial vehicle developed by Northrop Grumman. It is approximately 14.5 meters in length, and has wingspan of 40 meters, and a height of 4.7 meters. This aircraft, with a service ceiling of 18,288 meters, can fly continuously for up to 30 hours and has a range of 25,926 kilometers.

Figure 2.1 : RQ-4 Global Hawk.

The wingspan of this aircraft is 40 meters, and the chord length is 1.6 meters, resulting in an aspect ratio value is 25. The aspect ratio of this aircraft is quite high, and elastic effects can be seen in Figure 2.1.

This aircraft stands out as a High-Altitude Long-Endurance (HALE) class unmanned aerial vehicle in terms of its features and performance characteristics. This unmanned aerial vehicle is used for various purposes such as strategic reconnaissance and surveillance in terms of mission and operational areas. It is designed with a configuration that allows hardware and sensors to be easily attached and detached from the aircraft.

2.2 Aerodynamic Model

In this study, the RQ-4 Global Hawk aircraft has been selected. The aerodynamic model of this unmanned aerial vehicle is constructed using the ZONAIR program. ZONAIR solves using the linear small disturbance potential equation.

$$\bar{\beta}^2 \varphi_{\bar{x}\bar{x}} + \varphi_{yy} + \varphi_{zz} = 0 \text{ For subsonic flow} \quad (2.1)$$

$$-\bar{\beta}^2 \varphi_{\bar{x}\bar{x}} + \varphi_{yy} + \varphi_{zz} = 0 \text{ For supersonic flow} \quad (2.2)$$

$\bar{\beta} = \sqrt{|1 - M_{\infty}{}^2|}$: Compressibility effect constant

M_{∞} : is the freestream Mach Number, φ is the perturbation potential.

The Prandtl-Glauert transformation is applied to the potential flow equations in equation 2.1 to find a solution, making it a mathematical transformation method used to examine flows at subsonic speeds. This transformation encompasses the compressibility effects of the flow and calculates the pressure distribution. It is a set of equations commonly used in aerodynamic analysis and flow simulations at subsonic speeds.

$$\varphi_{xx} \pm \varphi_{yy} \pm \varphi_{zz} = 0 \quad (2.3)$$

Attached flow denotes a situation where the flow remains connected to the surface. Therefore, ZONAIR is unable to forecast flow separation. An irrotational flow refers to a flow pattern where there is minimal or no rotation of fluid particles. In supersonic conditions, the airflow ahead of a blunt-nose object exhibits significant rotation,

rendering ZONAIR's solution invalid. To address this, ZONAIR employs a correction method based on the precise Euler solution specifically for supersonic flows with blunt-nose bodies, correcting its potential flow solution. $M_\infty\ \tau \ll 1$ the thikness ratio (τ) of the configuration determines the validity of ZONAIR's solution, indicating that it is not applicable for transonic and hypersonic flows. Although ZONAIR primarily deals with inviscid flow, it includes a boundary layer option that utilizes the inviscid solution to calculate skin friction arising from the boundary layer.

The ZONAIR aerodynamic model is a high-order panel method, providing more accurate results compared to low-order panel methods. Examples of low-order panel methods include NLR-panel, Hess's code, VSAERO, and USSAERO. Since the ZONAIR method is a high-order approach, it applies the continuity condition in doublet distribution. This ensures continuity at common edges of high-order panels, contributing to the solution's consistency, and also prevents the formation of line vortex singularities.

ZONAIR also implements the Dirichlet boundary condition on the configuration surface,

$$\vec{n} \cdot \left(\vec{V} + \overrightarrow{V_\infty}\right)\Big|_{S=0} = 0 \tag{2.4}$$

$$\varphi|_{S=0} = Constant \tag{2.5}$$

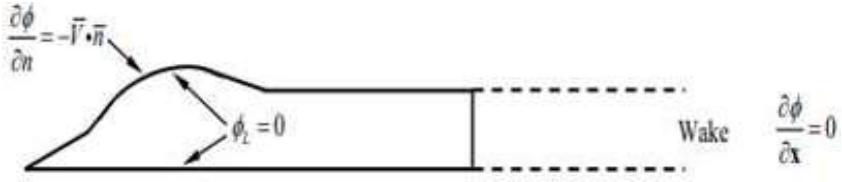

Figure 2.2 : Flow Boundary Condition [20].

The Dirichlet boundary condition basically means that when you're working with mathor models, you have to set a specific value at the edge of your system, like the outer edge which is shown Figure 2.2. This value has to be either a constant number or something you already know, like a function or equation. It's a rule that helps us solve math problems, especially when dealing with things like temperature, pressure, or how liquids or gases flow, by making sure we have clear starting points at the edges of our system.

ZONAIR creates boundary conditions to ensure tangency to the panel surfaces. When constructing the aerodynamic model, it sets specific conditions using its own cards to

determine whether the flow will form a wake or a vortex in that area, It creates the boundary condition using this knowledge. ZONAIR implements inviscid methods but aims to represent real flow by assuming an infinitesimally thin boundary layer. This thin layer is modeled using source and doublet sheets on panels. Flow above this layer is tangential to it, while below it, the velocity is set to zero $\left(\vec{\nabla}\varphi\right)\big|_{S=0} = 0$ to simulate the no-slip condition.

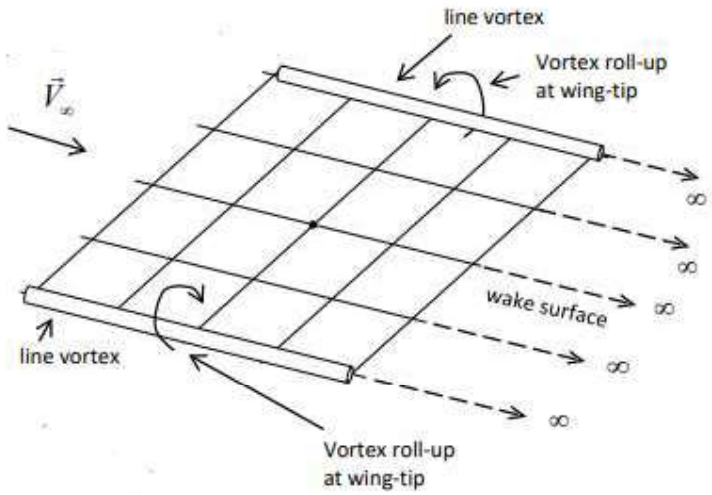

Figure 2.3 : Wake and vortex along trailing edge and tips [20].

The ZONAIR aerodynamic model shown in Figure 2.3 allows for the creation of a more complex, higher-order aerodynamic model compared to the NASTRAN flat plate aerodynamic model by considering wakes and vortices. For example, as shown in Figure 2.3, the ZONAIR aerodynamic model has the ability to use boundary conditions that create vortices in the tip region and boundary conditions that create wakes at the trailing edge. This feature allows the ZONAIR aerodynamic model to produce more accurate results.

The ZONAIR aerodynamic model of the RQ-4 Global Hawk aircraft has been carefully established to facilitate an in-depth analysis of the aircraft's aerodynamic performance. This model is constructed using a coarse mesh, which is designed to strike a balance between computational efficiency and the accuracy of aerodynamic predictions. The mesh is composed of both quadrilateral (quad) and triangular (tria) elements, allowing for a flexible yet precise representation of the aircraft's surface geometry. Notably, the mesh predominantly features quad elements, which are favored for their superior ability to maintain accuracy and stability in the aerodynamic

simulations. This thoughtful combination of quad and tria elements ensures that the model can reliably capture the complex aerodynamic characteristics of the RQ-4 Global Hawk, making it an essential tool for evaluating the aircraft's performance across various flight scenarios.

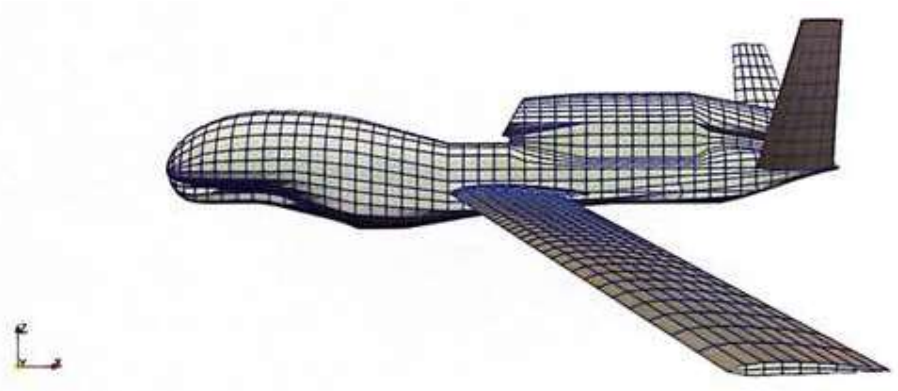

Figure 2.4 : ZONAIR aerodynamic model.

The aerodynamic model of the RQ-4 Global Hawk aircraft is developed using the CAD file of the aircraft available in the literature. The wing, fuselage, and tail of the aircraft is segmented into components, and these components is subdivided into the desired number of parts vertically and horizontally. A structured mesh is then generated using a Python code which is shown Figure 2.4. The ZONAIR aerodynamic solver provides more reliable results with structured meshing. Commercial meshing software is not used in creating the ZONAIR aerodynamic mesh because generating structured mesh with commercial software is challenging, hence the use of code for mesh generation.

As shown in Figure 2.5, the CAD file is used to separate the aircraft into its components using a Python script. These components, such as the wing, tail, and fuselage, are then subdivided into spanwise and chordwise quad elements. Afterward, the components are merged together, and a structured mesh is generated.

In this study, one of the objectives is to speed up the jig shape optimization process. Consequently, the ZONAIR aerodynamic model is modeled with only 3320 elements. The ZONAIR aerodynamic mesh is then generated with a total of 3411 nodes. As seen in Figure 2.4, a structured mesh has been applied, meaning that most of the mesh elements are quadrilateral. Using a structured mesh in this manner is beneficial for both reducing solution time and improving solution convergence. Additionally, this

approach ensures that computational processes are more stable and reliable. This setup also facilitates easier mesh management and better accuracy in the simulation results.

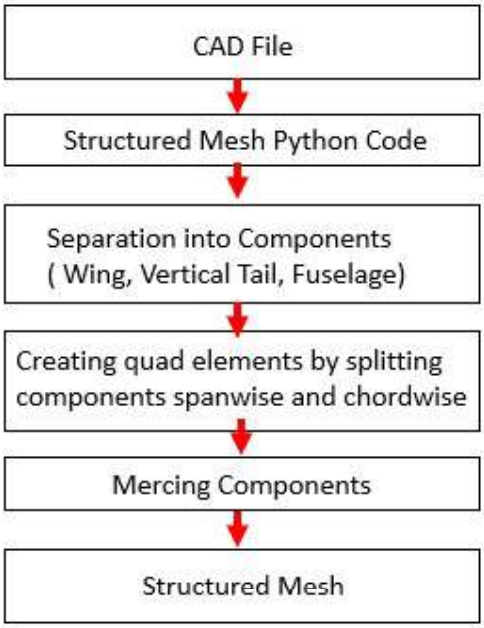

Figure 2.5 : Creating sructured mesh flowchart.

Up to this point, was discussed the meshing process of the ZONAIR aerodynamic model. Because ZONAIR is a high-order panel method, it requires introducing boundary conditions to ensure that the model behaves realistically. These boundary conditions are introduced to the model using ZONAIR cards. The aerodynamic model is created by utilizing these specific cards for areas that create wakes and vortices in real-life scenarios which is shown in Figure 2.6.

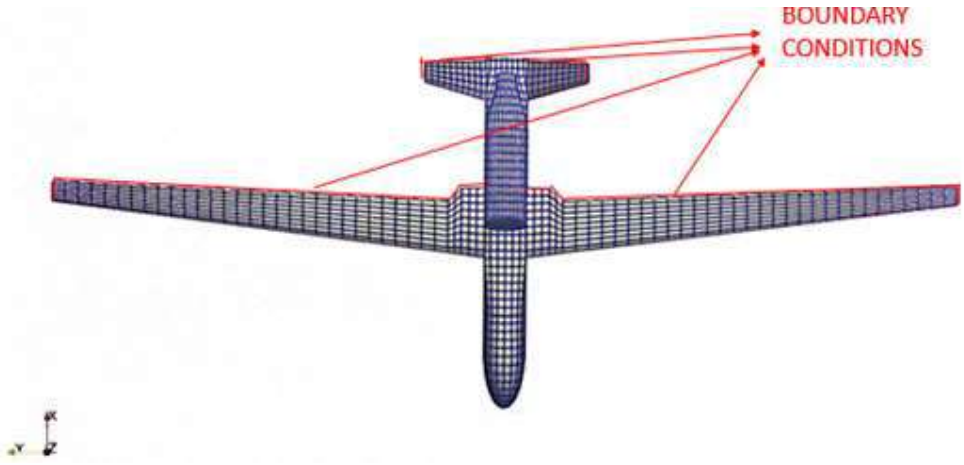

Figure 2.6 : ZONAIR aerodynamic model boundary conditions.

Boundary condition cards based on appropriate flow physics are used in areas marked with red lines. For instance, in real life, a wake forms behind the wing, so a wake boundary condition card is used. Similarly, vortices form at the wing and vertical tail tip sections, and a vortex boundary condition card is used to simulate these areas

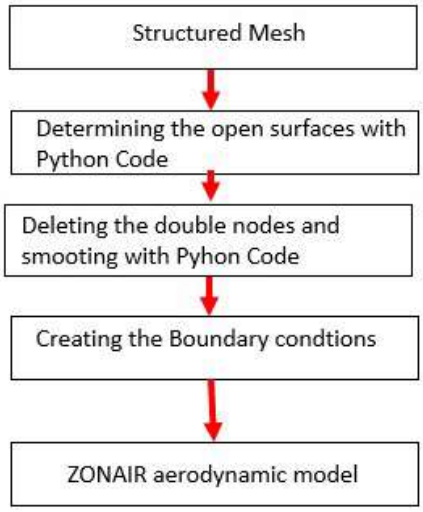

Figure 2.7 : Creating ZONAIR aerodynamic model flowchart.

The ZONAIR aerodynamic model is created based on the steps highlighted in Figure 2.7. Now, the ZONAIR aerodynamic model of the RQ-4 Global Hawk unmanned aerial vehicle is ready. The RQ-4 Global Hawk aircraft is generally optimized for Mach 0.6 and at an angle of attack around 6 degrees, and it generally operates its life under these flight conditions. Using the ZONAIR solver, a solution is obtained for these conditions, and Cp contours are drawn in Figure 2.8, Figure 2.9 anad Figure 2.10. This analysis offers a detailed understanding of the UAV's aerodynamic performance under its typical operational conditions by evaluating Cp contours and other parameters at Mach 0.6 .

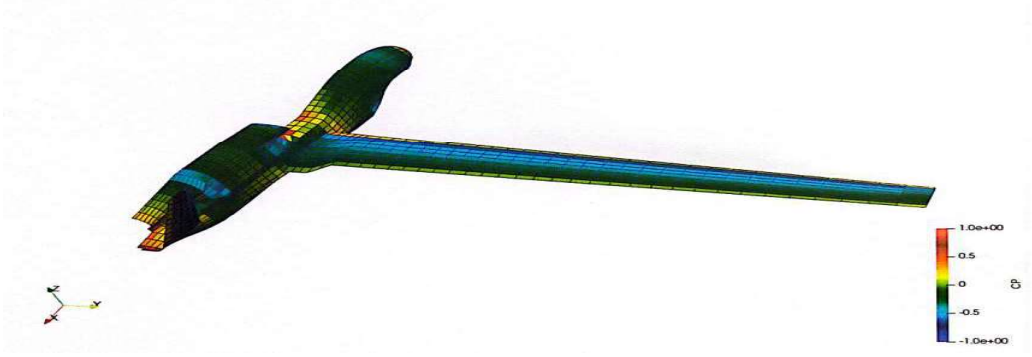

Figure 2.8 : MACH:0.6, AoA: 6 degree, Pressure contours- izometric view.

Figure 2.9 : MACH:0.6, AoA: 6 degree , Pressure contours- top view.

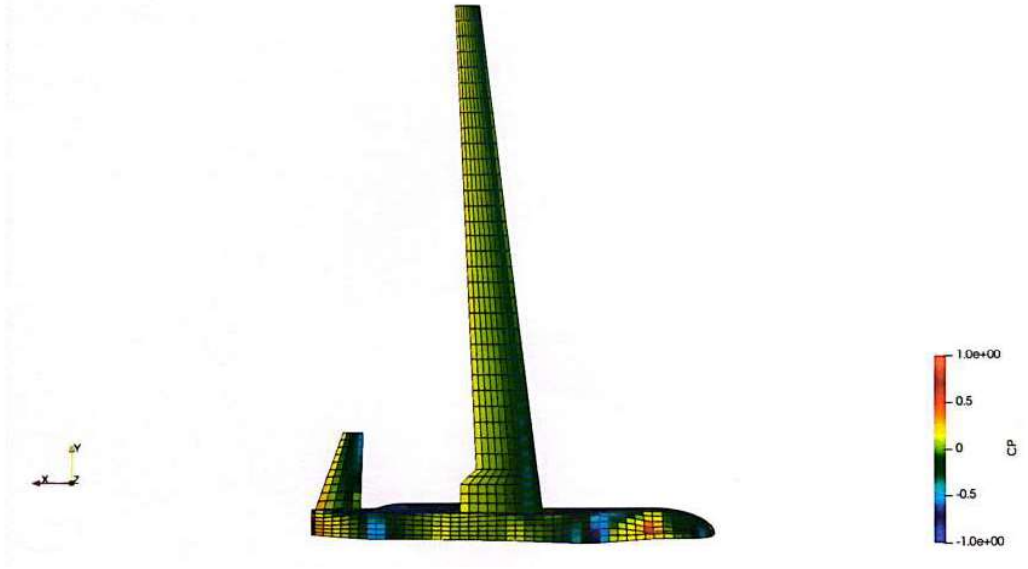

Figure 2.10 : MACH:0.6, AoA: 6 degree , Pressure contours- bottom view.

After this, the lift coefficient-angle of attack graphs are plotted for three different Mach numbers namely 0.3, 0.6, and 0.9 for the RQ-4 Global Hawk aircraft. Due to the structured mesh and the low number of mesh elements in the ZONAIR aerodynamic model of the RQ-4 Global Hawk aircraft, the solution time is around 46.5 seconds. The solution time being below one minute indicates a cost-effective model. The ZONAIR aerodynamic model of the RQ-4 Global Hawk aircraft has become a fast model that we can be easily used in design and optimization models. Consequently,

the ZONAIR aerodynamic model of the RQ-4 Global Hawk has become an efficient tool that can be easily integrated into design and optimization processes.

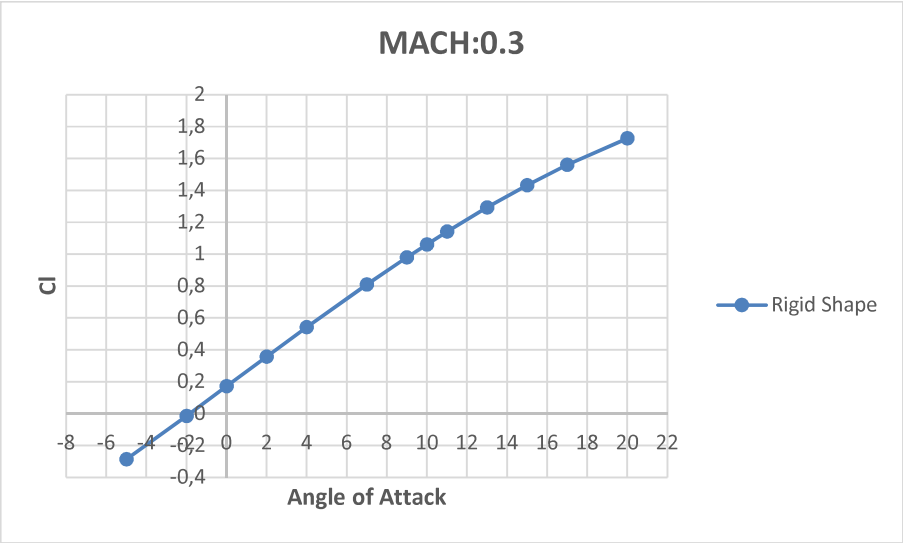

Figure 2.11 : Mach: 0.3, Lift coefficient vs Angle of Attack.

Solutions have been obtained for a rigid aircraft in the ZONAIR solver at Mach values of 0.3, 0.6, and 0.9. These results provide valuable data on the aerodynamic performance across different mach numbers, aiding in the assessment and optimization of the aircraft's design under varying flight conditions.

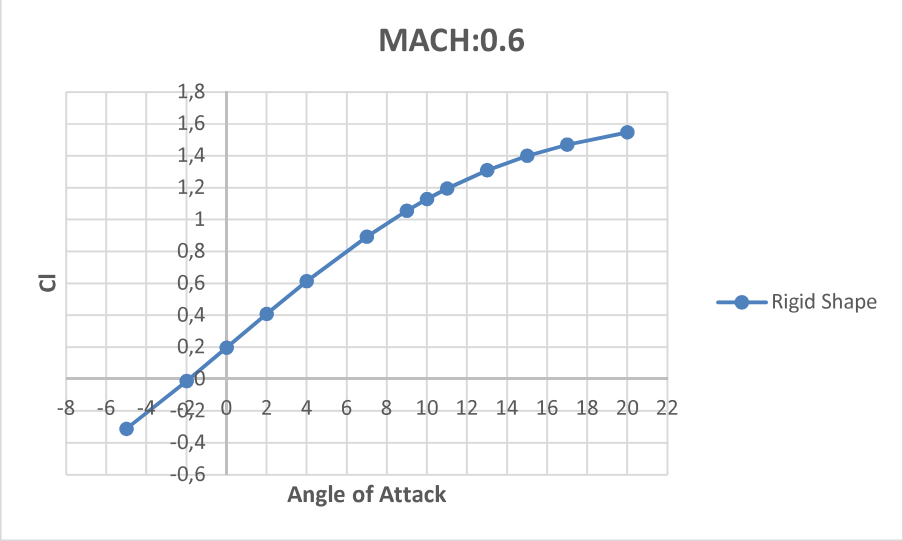

Figure 2.12 : Mach: 0.6, Lift coefficient vs Angle of Attack.

The Mach numbers presented in Figures 2.12 and 2.13 represent significant flight conditions for this UAV. This is because the UAV typically operates within a Mach

range of 0.3 to 0.6. For this particular UAV, the majority of its operational flights are conducted at a Mach number of 0.6. As shown in Figure 2.13, this aircraft is capable of achieving high angles of attack. According to literature research, this UAV operates at a Mach number of 0.6 with an angle of attack around 4 degrees, and it conducts its cruising flight at these altitudes.

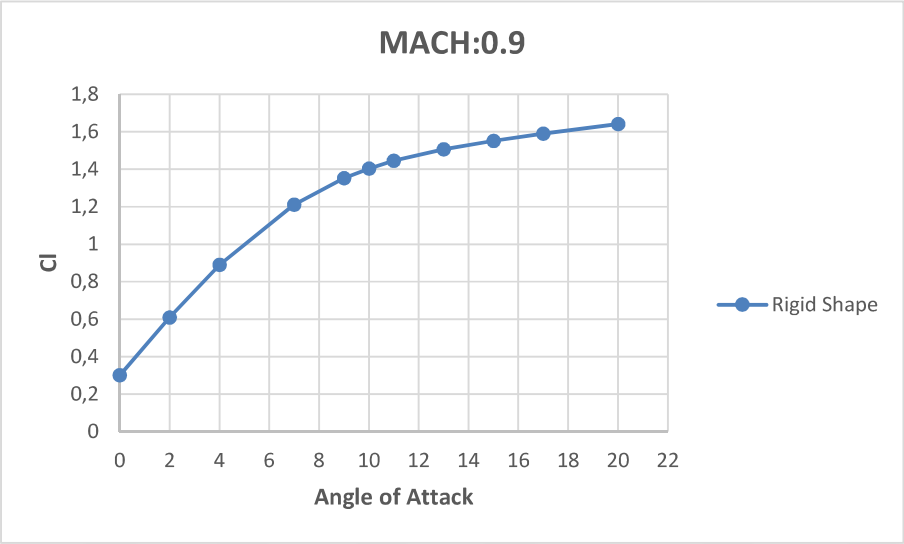

Figure 2.13 : Mach: 0.9, Lift coefficient vs Angle of Attack.

Figures 2.11, 2.12, and 2.13 show lift coefficient versus angle of attack graphs for Mach numbers 0.3, 0.6, and 0.9. Solutions were obtained based on the flight envelope of the RQ-4 Global Hawk aircraft. The solution time for each data point is below one minute for the rigid aircraft. Accurate simulation of the flight is essential for predicting jig shape and Flight shape correctly, meaning our aerodynamic solutions must be realistic. Therefore, the aerodynamic model needs to be validated. Aerodynamic validation will be conducted in the next section.

2.3 RQ-4 Global Hawk ZONAIR Aerodynamic Model Validation

Aerodynamic validation is typically carried out using wind tunnel or flight data. For comparative purposes, flight data is considered the most accurate, followed by wind tunnel data, CFD solutions, and lastly panel methods in terms of accuracy. Comparing aerodynamic data from wind tunnel with flight data is somewhat easier because flight data includes effects from inlets, engines, and nozzles. Particularly, observing engine effects in wind tunnel tests is quite challenging.

Eaton and Woolf have published flight data for the RQ-4 Global Hawk aircraft, where they compared their CFD results with the actual flight data. The published paper contains the flight data for the RQ-4 Global Hawk aircraft. This article provided an opportunity to validate the ZONAIR aerodynamic model. In these studies, the focus was on how to eliminate noise from flight data, what types of filters should be used, and how to transform flight data into meaningful information. These topics were thoroughly addressed to enhance the reliability and accuracy of the aerodynamic analysis [21].

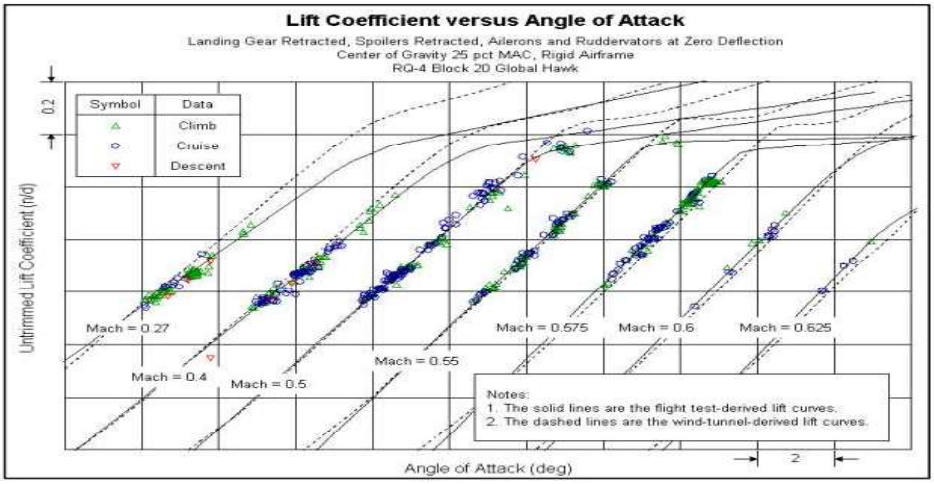

Figure 2.14 : RQ-4 Global Hawk flight data [21].

The ZONAIR solutions are obtained for the Mach values found in the flight data provided in Figure 2.14.

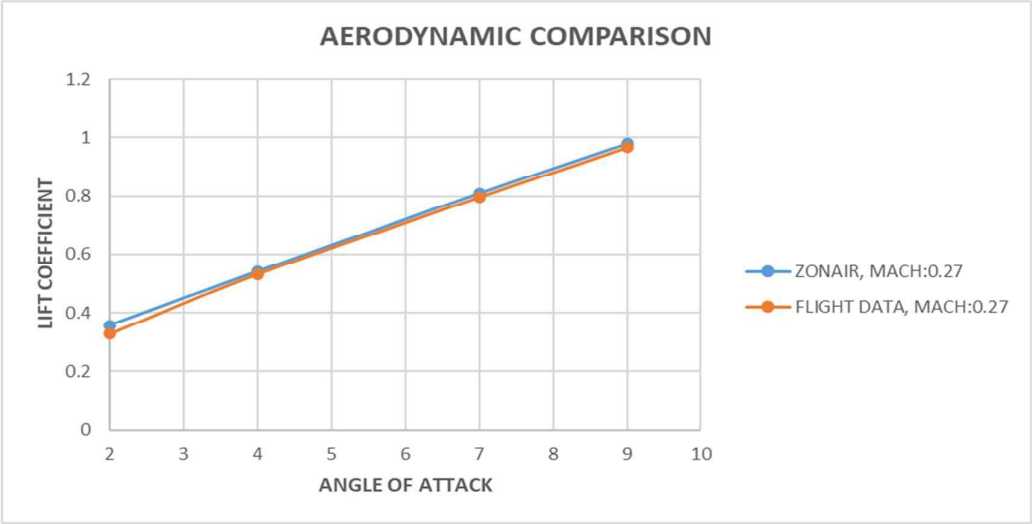

Figure 2.15 : Mach: 0.27, ZONAIR result - Flight data comparison.

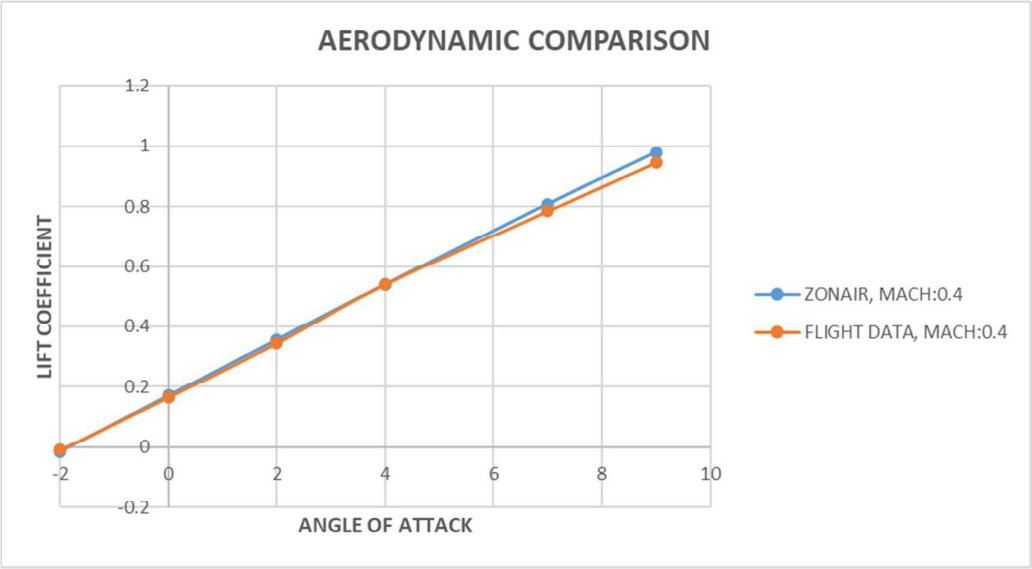

Figure 2.16 : Mach: 0.4, ZONAIR result - Flight data comparison.

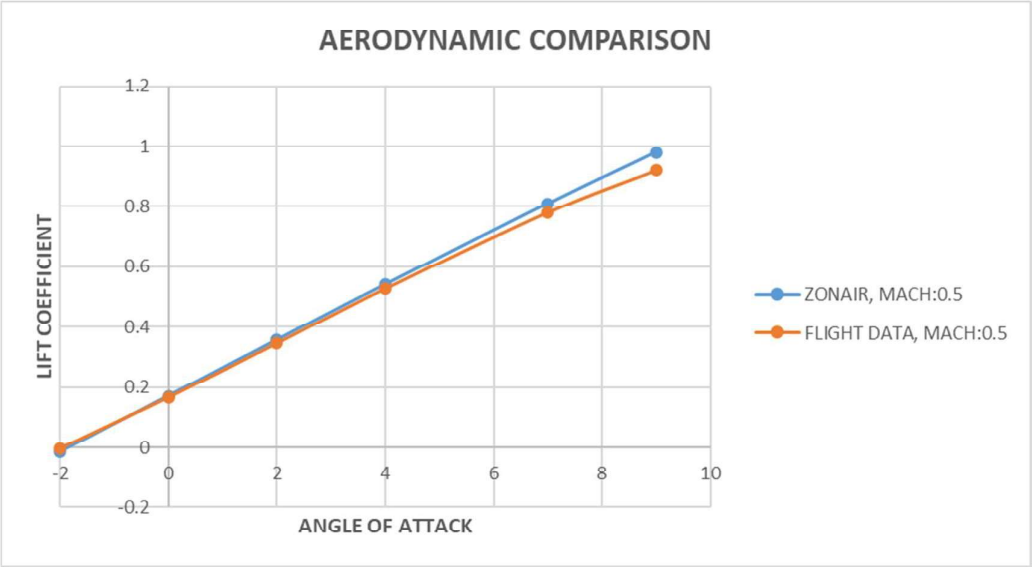

Figure 2.17 : Mach: 0.5, ZONAIR result - Flight data comparison.

Flight data and ZONAIR solutions were compared at different angles of attack and Mach values, as seen in Figures 2.15, 2.16, 2.17 and 2.18. ZONAIR solution starts to diverge with flight data at high angles of attack, the reason for this will be explained in detail, the graph of mach number 0.6 is shown in Figure 2.18. Comparison of lower Mach values is given in Figure 2.15, 2.16. When looking at low Mach values, the curves overlap each other. Since these comparisons are real flight data using the panel method, overlapping values indicate the success of the model. Data from the flight data

graph published in the article was extracted using one of the pixel engineering techniques known as the digitization method.

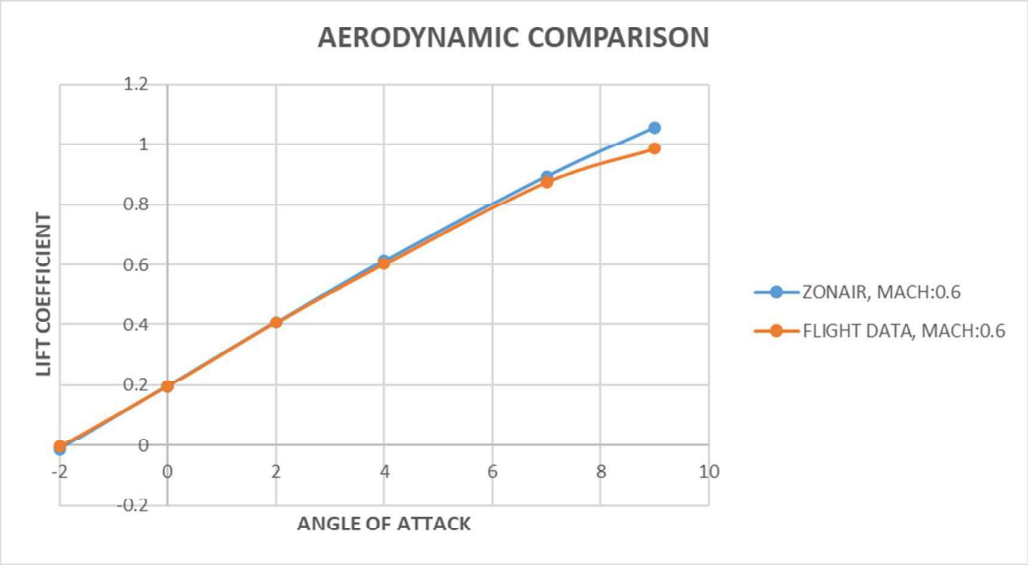

Figure 2.18 : Mach: 0.6, ZONAIR result - Flight data comparison.

The flight data of the RQ-4 Global Hawk aircraft has been compared with the ZONAIR aerodynamic model solutions. Lift coefficient values for different angles of attack at Mach values of 0.27, 0.4, 0.5, and 0.6 are compared with the flight data avaible in the literature. Upon examining each value individually, it is evident that the accuracy of the RQ-4 Global Hawk aircraft's ZONAIR aerodynamic model is very high. A closer look at the graphs reveals minimal differences at high and very low angles of attack, which is normal due to the effects of the inlet, engine, and nozzle. When comparing these two datasets, the results are very close for some angles of attack where the lift coefficients are nearly identical. The established ZONAIR aerodynamic model demonstrates a high level of success in this comparison, with each solution value taking less than a minute. The validation of the RQ-4 Global Hawk aircraft's ZONAIR aerodynamic model has been achieved, making it suitable for use in aeroelastic analyses with confidence.

2.4 Structural Model

The RQ-4 Global Hawk aircraft being a military plane, there is no literature available on its natural frequencies and mode shapes. However, a structural model is developed through reverse engineering based on a literature review. This process involves

obtaining the CAD model of the RQ-4 Global Hawk aircraft and using a Python code to break it down into different components. The volumes of each component, such as the wing, fuselage, and vertical tail, are calculated proportionally. This allows for determining the weight distribution, with the wing weighing 3645 kg, fuselage 2298 kg, and vertical tail 301 kg, resulting in an empty weight of 6244 kilograms for the aircraft.

The aerodynamic mesh created for the ZONAIR aerodynamic model is converted to a PATRAN structural mesh using a Python code. Properties are assigned to shell elements, and values close to actual stiffness are entered. In this study, the focus will be on aerodynamic optimization rather than structural optimization, specifically regarding jig shape optimization. One of the goals of this study is to make jig shape optimization faster and more practical. It's important to note that there may be an increase in weight in the structural aspect of jig shape optimization, which is an undesirable outcome. that needs to be carefully managed. Additionally, addressing this potential weight increase will be crucial to achieving a balance between aerodynamic efficiency and structural integrity.

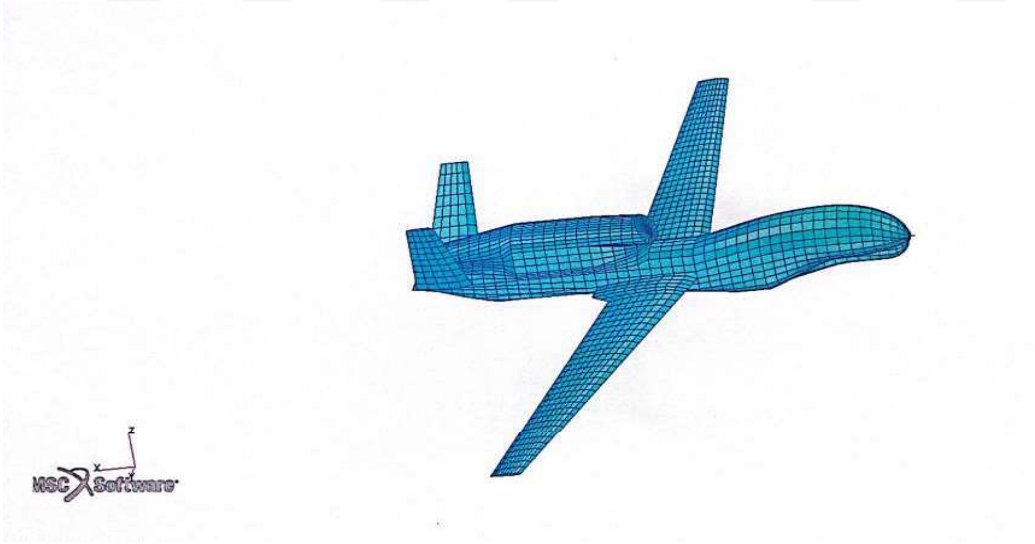

Figure 2.19 : RQ-4 Global Hawk FEM model.

The structural FEM model of the RQ-4 Global Hawk aircraft was set up in PATRAN. It consists of 4014 elements and is created using a total of 3285 nodes throughout the model. As seen in Figure 2.19, the structural mesh, like the aerodynamic mesh, is a structured mesh. In other words, it is quad-dominant. In the structural mesh of this

aircraft, surface information with stiffness values is assigned to the surfaces. The small number of elements in this model has increased the solution speed.

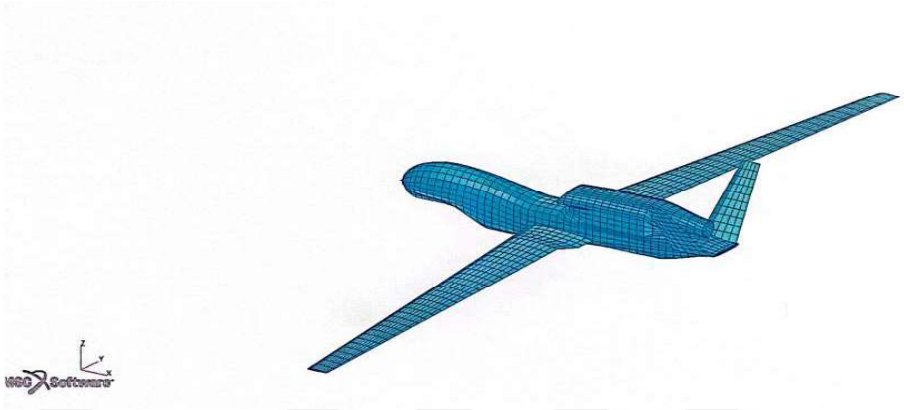

Figure 2.20 : RQ-4 Global Hawk FEM model.

The structural FEM model of the RQ-4 Global Hawk aircraft is displayed from different angles in Figures 2.20 and 2.21. These figures provide a comprehensive view of the model's details and dimensions, facilitating a better understanding of UAV.

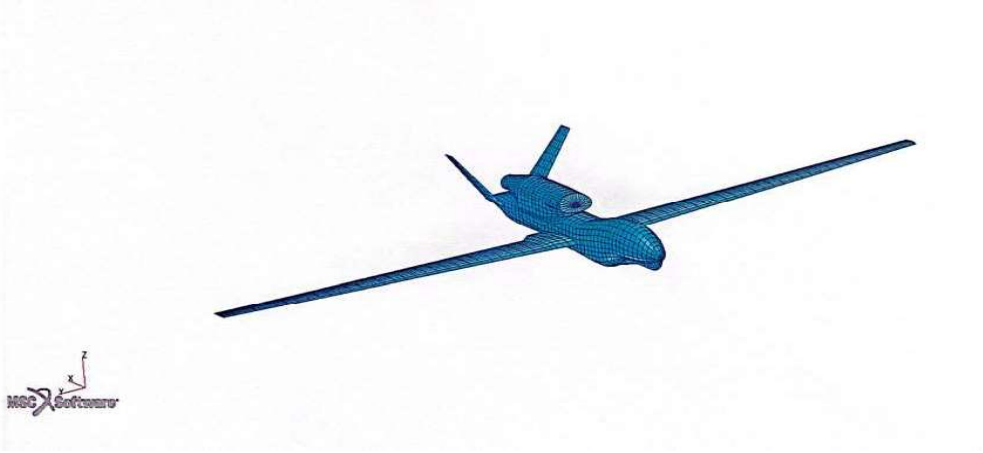

Figure 2.21 : RQ-4 Global Hawk FEM model.

In jig shape optimization, the main focus is on the wing components, so especially the wing's natural frequencies and mode shapes of the wing were extracted. The first 6 modes of the aircraft are rigid body modes. Among the subsequent natural frequencies and mode shapes, wing modes are identified, which are crucial for understanding the wing's dynamic behavior and ensuring its performance under different flight conditions. Accurate identification of these modes helps in refining the jig shape to enhance aerodynamic efficiency while maintaining structural stability.

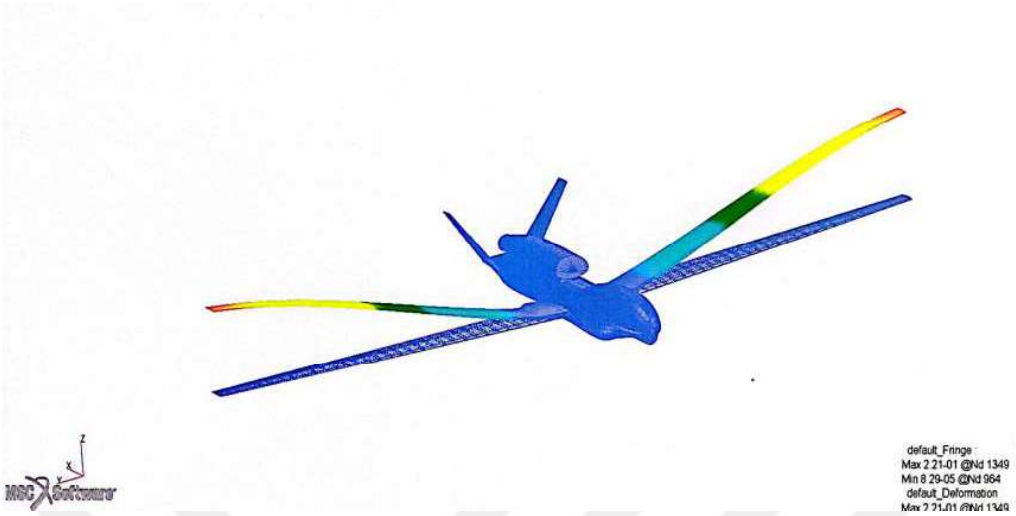

Figure 2.22 : Wing First Bending mode.

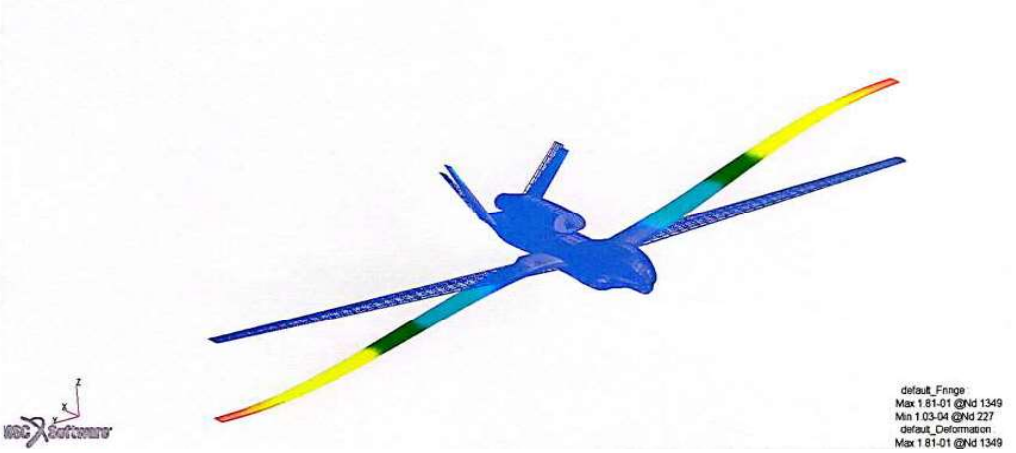

Figure 2.23 : Wing Antisymetric bending + 1st Torsion mode shape.

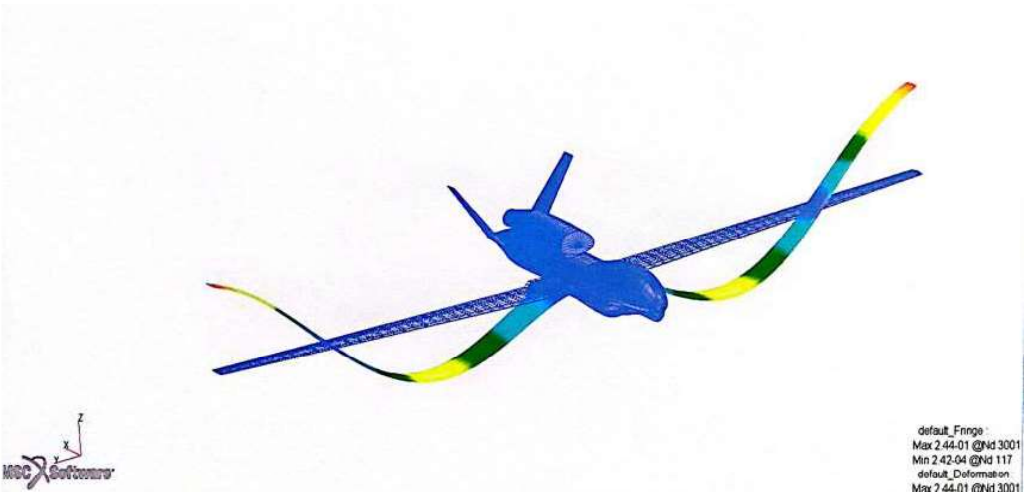

Figure 2.24 : Wing Second Bending mode shape.

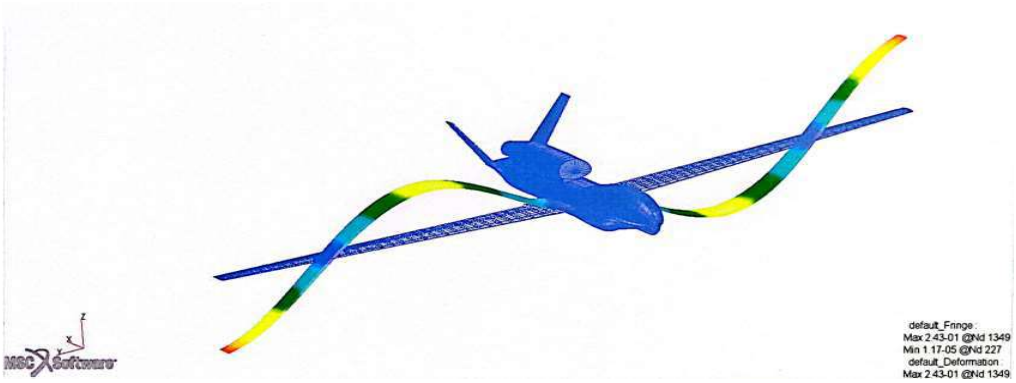

Figure 2.25 : Wing Antisymetric Second Bending mode shape.

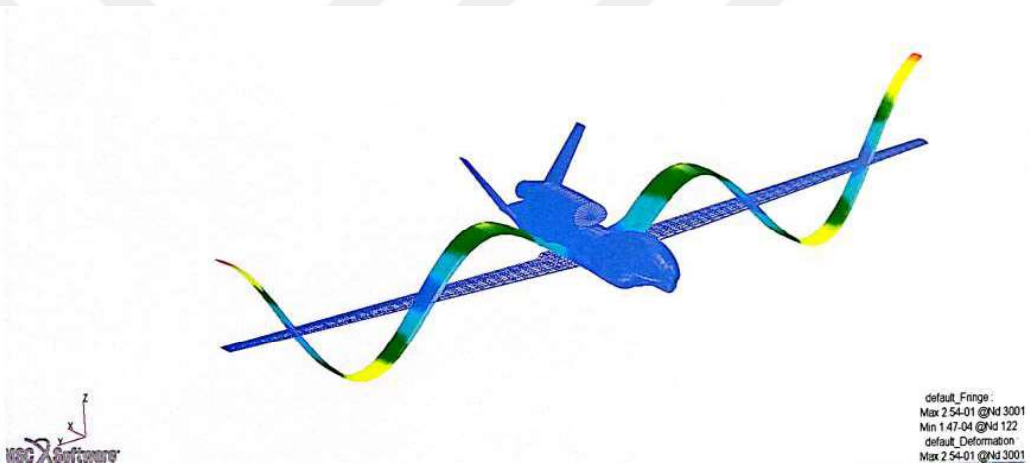

Figure 2.26 : Wing Third Bending mode shape.

Table 2.1 : Natural frequency response of the aircraft wing**.**

Mode Shape	Natural Frequency
Wing Antisymetric Second Bending Mode Shape	42.15 Hz
Wing Antisymetric bending + 1st Torsion Shape	16.02 Hz
Wing Second Bending Mode Shape	31.07 Hz
Wing Third Bending Mode Shape	47.98 Hz
Wing First Bending Mode	11.37 Hz

The FEM model of the RQ-4 Global Hawk aircraft is set up in PATRAN, and Modal analysis is performed using the NASTRAN structural solver with the Sol 103 module, identifying the natural modes related to the wing. This analysis provides critical

insights into the wing's dynamic behavior and vibration characteristics, essential for optimizing its performance and structural integrity. Table 2.1 displays the names and frequency values of the mode shapes. Figure 2.22 shows the wing first bending mode, Figure 2.23 depicts the wing antisymetric bending + 1st torsion mode shape, Figure 2.24 presents the wing second bending mode shape, Figure 2.25 illustrates the wing antisymetric second bending mode shape, and Figure 2.26 showcases the wing third bending mode shape.

2.5 Aero-Structural Model

The aero-structural model, consisting of 4014 elements in the structural FEM model and 3320 elements in the aerodynamic model, is created according to the ZONAIR solver, using the spline method to couple the two models. Specifically, the 3D spline method is employed to transfer aerodynamic forces generated in three-dimensional aerodynamic panels to the panels in the 3D FEM structural model, thus creating an aero-structural coupling model.

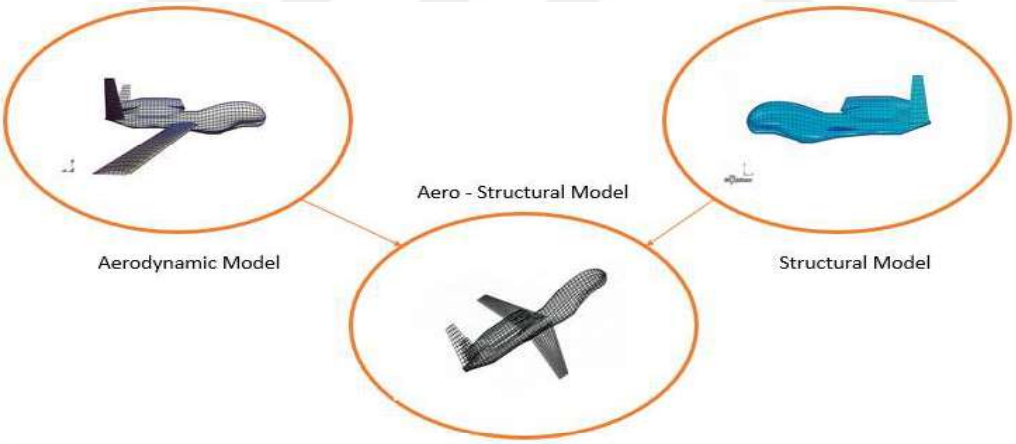

Figure 2.27 : ZONAIR Aero-Structural model.

Aero-structural modeling attempts with FSI involve creating meshes on the order of millions of elements. However, the ZONAIR aero-structural model comprises a total of 7334 elements which is shown iin Figure 2.27. Due to its relatively low number of elements and the structured mesh nature of both the aerodynamic and structural models, the nodes among mesh elements can communicate with each other easily. These features collectively enable the aero-structural model to achieve very fast solutions.

Jig shape optimization involves going through a long iterative process. One of the objectives of this thesis is to shorten this lengthy iteration time. Since jig shape optimization is a topic within static aeroelasticity, the equation set for static aeroelasticity using the ZONAIR solver is generally as follows.

$$\left[[\mathrm{K}] - \mathrm{q}_\infty\,[\mathrm{G}]^{\mathrm{T}}[\mathrm{AIC}][\mathrm{G}]\right]\{\mathrm{X}\} = \mathrm{q}_\infty \mathrm{F}_{\mathrm{R}} - [\mathrm{M}]\{\ddot{\mathrm{u}}\} \tag{2.6}$$

$[K]$: Stiffness matrix from Nastran

$[G]$: Spline matrix by ZONAIR

$[G]^T$: Spline matrix transpose by ZONAIR

$[AIC]$: Aerodynamic Influence Coefficient matrix by ZONAIR

$\{X\}$: Structural deformation

F_R: Mapped rigid loads

$[M]$: Mass matrix from Nastran

$\{\ddot{u}\}$: Aircraft rigid body accelerations

Total flexible aerodynamic loads,

$$\mathrm{F}_{\mathrm{total}} = \mathrm{q}_\infty \mathrm{F}_{\mathrm{R}} + \mathrm{q}_\infty\,[\mathrm{G}]^{\mathrm{T}}[\mathrm{AIC}][\mathrm{G}]\{\mathrm{X}\} \tag{2.7}$$

Using these equation sets, both rigid and elastic solutions are obtained. Several solutions have been obtained using the aero-structural model with the ZONAIR solver. ZONAIR solver operates in the background with a theory similar to NASTRAN solver. However, ZONAIR employs updated iteration methods and aeroelastic theories. Upon reviewing the ZONAIR user manual, many models have been validated with wind tunnel data.

This validation demonstrates the accuracy and reliability of ZONAIR in predicting aerodynamic and aeroelastic behaviors, confirming its robustness as a tool for analyzing and optimizing aircraft performance under a range of flight conditions. The successful validation with wind tunnel data highlights ZONAIR's capability to provide precise and consistent results, which is crucial for effective design and performance evaluation. By incorporating advanced iteration methods and aeroelastic theories, ZONAIR ensures that the models produced not only reflect realistic aerodynamic and structural interactions but also align with practical requirements in aircraft design. This comprehensive approach supports detailed performance analysis, allowing for more informed decision-making and optimization in the development of advanced aerospace technologies. Based on the literature review, it was found that the RQ-4 Global Hawk

aircraft flies at a Mach 0.6 with an angle of attack of 6 degrees. A more detailed literature review reveals that real flight photographs of this flight condition have been shared in Figure 2.28. Figures 2.3 and 2.4 clearly show the difference between the flight shape and rigid shape at a Mach number of 0.6.

Figure 2.28 : Mach:0.6 AoA:6 degree, ZONAIR result -Izometric View.

The flight condition for the RQ-4 Global Hawk aircraft is set at Mach 0.6 and AoA 6 degrees. The solution time for the entire [AIC] matrix is 8 minutes, and the solution time for one flight condition is 38 seconds.

Figure 2.29 : Mach:0.6 AoA:6 degree, ZONAIR result -Front View.

Figure 2.29 shows the rigid and elastic solutions of the aircraft at a Mach number of 0.6 and an angle of attack of 6 degrees. This comparison provides insight into how the aircraft's performance differs under rigid and elastic conditions, highlighting the effects of aeroelastic interactions on its aerodynamic behavior. The detailed visualization helps in understanding the influence of structural flexibility on the overall flight dynamics and design optimization. Additionally, this comparison underscores

the importance of considering both rigid and elastic analyses in optimizing aircraft design for real-world operational conditions.

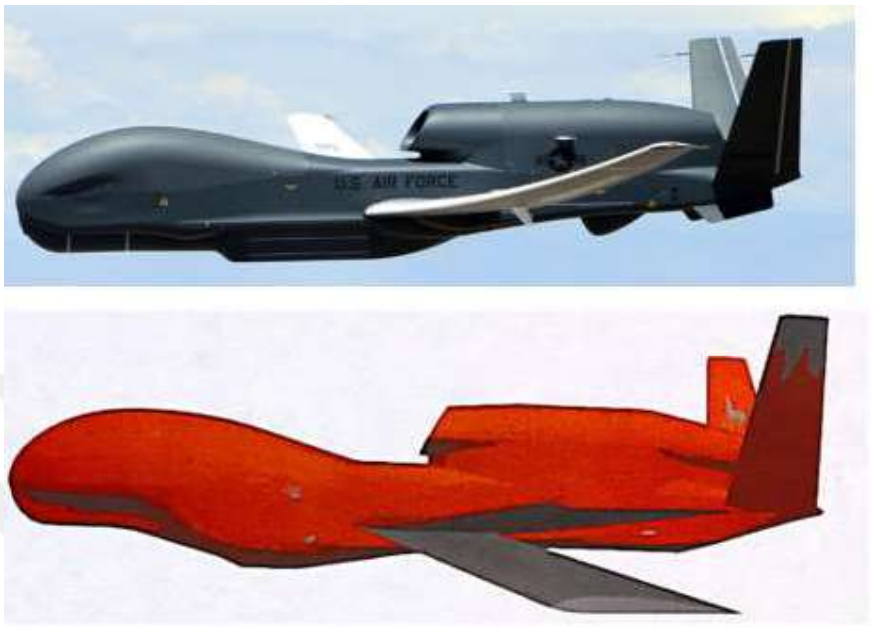

Figure 2.30 : The photo at the top: actual flight, at the bottom: ZONAIR solution.

The condition of Mach-0.6 and AoA of 6 degrees is compared between the ZONAIR solution and an actual flight photograph in Figure 2.30. A closer examination of this figure revealed nearly identical trends with respect to wing bending and twisting.

Figure 2.31 : The photo at the left: actual flight, at the right: ZONAIR solution.

When looking at Figure 2.31, a comparison between different angles of the aircraft's flight photograph and the ZONAIR solution reveals similar trends. The wing's bending and twist shapes in the air appear to resemble each other. As seen in Figure 2.30, elastic effects are also highly significant on the wings in real life.

3. EXTERNAL SHAPES IN THE LIFE-CYCLE OF UAV

Unmanned Aerial Vehicles are complex industrial products. The shape of the UAVs, which is important to all parties involved, is a key characteristic. Throughout the lifecycle of UAVs, different shapes are used for various states and purposes of the aircraft.

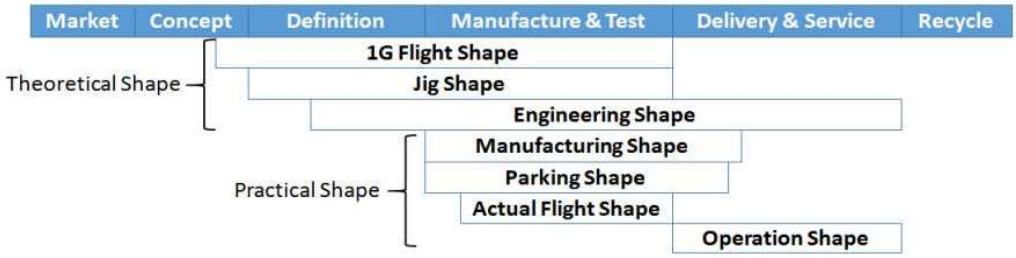

Figure 3.1 : Different external shapes in their corresponding application phases [7].

Although not widely known, aircraft have numerous shape definitions that evolve over time. As shown in Figure 3.1, aircraft have seven shape definitions. For a highly efficient aircraft design, every detail must be right from the conceptual stage. This is because aircraft design is a complex product, requiring multidisciplinary thinking throughout the design process.

3.1 Flight Shape

The flight shape describes how an airplane looks during regular cruising with a specific 1G load. This load condition is set for a particular cruising speed, altitude, and weight. The 1G flight shape is crucial for aerodynamic design and analysis, using inputs, performance goals, and technical limits. It starts in the conceptual design phase and gets finalized in the definition phase after going through optimization stages. Freezing the 1G flight shape at various stages helps evaluate it effectively. Once frozen, it remains unchanged throughout testing.

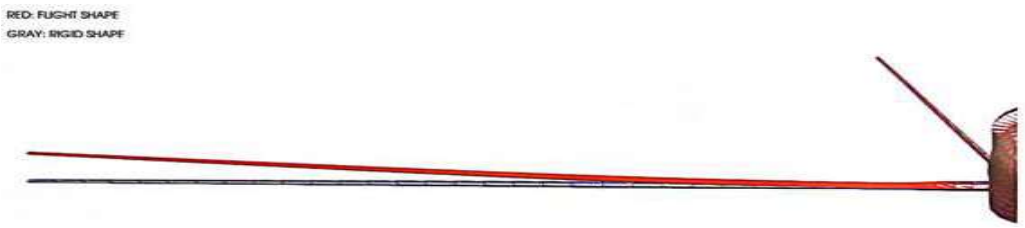

Figure 3.2 : Mach: 0.6, AoA: 6 degree, Flight and Rigid shape.

A solution with Mach 0.6 and an angle of attack of 6 degrees is obtained, as shown in Figure 3.2. The ZONAIR solver is used to determine the rigid shape and flight shape of the RQ-4 Global Hawk aircraft. The bending and twist values shown in Section 2.5 are considered realistic.

3.2 Jig Shape

The usual approach in aircraft aerodynamic design is to optimize for maximum efficiency during cruising, assuming a rigid structure. However, aerodynamic forces can cause the cruise shape to deviate from the desired form. To solve this problem, designing a jig shape that reverts back to the desired cruise shape during flight is a viable solution. Jig shape represents the aircraft's theoretical form unaffected by factors like weight, lift, and aerodynamics. It plays a crucial role in defining the aircraft and serves as the foundation for subsequent design processes. Derived from the 1G flight shape, certain sections of the jig shape, like the fuselage and tail, remain unchanged. However, components like the wing, high lift devices, flap fairing are transformed from the 1G flight shape to fit the jig shape. Additionally, the jig shape might incorporate pre-deformation to account for aerodynamic effects.

The formulas used for calculating the jig shape are as follows: Cp_{jig} Incremental pressure coefficient due to the structural deformation which can be computed from the aerodynamic influence coefficient (AIC) matrix.

Assume Cp_{jig} represents the pressure coefficients targeted for the jig shape. Then, the variance lies in the pressure coefficients assigned to the desired cruise shape, denoted as Cp_{cruise} .

$$\{Cp_{cruise}\} - \{Cp_{jig}\} = [AIC][\varphi_e]\{\xi\} \tag{3.1}$$

$$\{Cp_{cruise}\} = [AIC][\varphi_e]\{\xi\} + \{Cp_{jig}\} \tag{3.2}$$

$$[[K_{ee}] - q_\infty[Q]\{\xi\} = q_\infty[\varphi_e]^T\left[S_{kj}\right]^T\{Cp_{jig}\} \tag{3.3}$$

$$\{\Xi\} = [A]\{Cp_{jig}\} \tag{3.4}$$

$$[A] = q_\infty[[K_{ee}] - q_\infty[Q]]^{-1}[\varphi_e]^T\left[s_{k_j}\right]^T \tag{3.5}$$

$[K_{ee}]$ is the generalized stiffness matrix of the elastic modes.

$[Q] = [\varphi_e]^T[AIC][\varphi_e]$ is the generalized aerodynamic force matrix.

S_{kj} is the integration matrix to convert pressure to forces

q_∞ is the dynamic pressure

$$Cp_{jig}(M,a) = Cp_{cruise}(M,a) - [AIC](M,a)][\phi_e]\{q_e\} \quad (3.6)$$

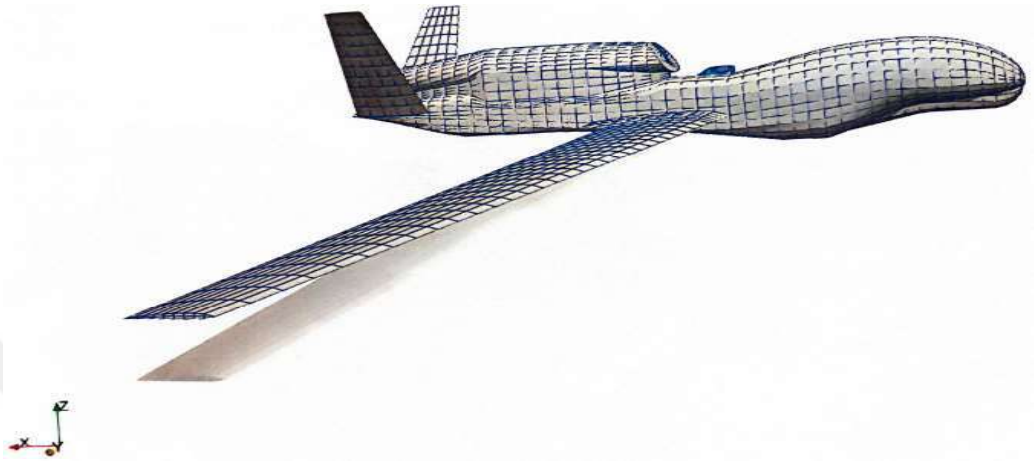

Figure 3.3 : Mach: 0.6, AoA: 6 degree, Jig shape.

The equations used for calculating the jig shape using the ZONAIR solver are provided in Figure 3.3.. These equations are utilized to compute the jig shape. When calculating the jig shape pressure, it is evident from the equations above that the jig shape pressure is derived from the cruise shape calculations. Therefore, jig shape calculations are lengthy and challenging. For wings under the cruise condition, the wings twist downward due to aeroelastic effects. Therefore, to ensure the Jig shape under cruise condition can deform back to cruise shape, the jig shape must have build-in twist-up wings. The twist-up wings of jig shape generate higher lift than cruise shape.

3.3 Engineering Shape

Jig shape is the initial perfect shape of the aircraft. It guides the detailed design work by the aerodynamic, structural, and system teams. However, this perfect shape becomes less perfect due to factors like skin overlaps, antenna installations, and reinforced structures. This less perfect shape is then used as the theoretical model for the aircraft, known as the engineering shape. The engineering shape is a theoretical representation that needs to match the actual detailed product shape [7].

3.4 Manufacturing Shape

Once the design phase is complete, the aircraft is built by the manufacturing team using the drawings. During this process, errors in manufacturing and changes caused by the aircraft's weight lead to a new shape known as the manufacturing shape. This shape reflects the actual appearance of the aircraft but may have errors. To manage these errors, specific tolerance controls are necessary during manufacturing [7].

For both component-level and overall aircraft-level considerations, tolerances are crucial. In terms of engineering shape, partial tolerances include aspects like profile, waviness, roughness, and fasteners. On the overall tolerance level, examples include twist, incidence, dihedral, and sweep.

3.5 Parking Shape

After aircraft manufacturing, it bends due to gravity when supported by landing gear, forming the parking shape. This shape is measured but typically only in key areas, not the entire exterior. It's used to fine-tune structural aspects and create manuals, like specifying ground clearance in repair manuals. The parking shape is established post-manufacturing and remains until early delivery [7].

3.6 Actual Flight Shape

The actual flight shape is determined by measuring the aircraft during flight, much like the parking shape. It does not cover the entire aircraft but focuses on key areas like wing deformation, door openings, and gaps around moving parts. Measuring the actual flight shape helps evaluate the design compared to the jig shape and 1g flight shape for improvements. This shape is established after the first flight and remains until the testing phase concludes and it remains same [7].

3.7 Operation Shape

The shape of the aircraft during airline operation is known as the operation shape. It starts from delivery to the customer and remains in use until the aircraft is decommissioned. The operation shape is not fixed; it evolves over time as the aircraft ages, a process called deterioration. Factors like natural aging, incorrect operation,

inadequate maintenance, and repairs contribute to deterioration. This degradation mainly affects aerodynamic drag, leading to higher fuel consumption. For instance, the loss of a high-density paint coating over 1 m^2 of the wing's leading edge can increase fuel consumption by over 2500 US gallons annually for a single-aisle aircraft. With respect to economic factors, monitoring the operation shape is crucial, focusing on issues like poor gap sealing, paint deterioration, external patches, and misaligned doors. Deciding when to address these concerns balances maintenance costs against fuel efficiency, guided by extensive research data from CFD methods, wind tunnel tests, and airlines' performance [7].

3.8 Flight Shape Results

The purpose of this study was to evaluate the aerodynamic differences between the rigid shape and the elastic shape before the jig shape optimization process.

MACH :0.3

MACH	Rigidity	ALPHA	CL
0.3	Elastic	0	0.16021
0.3	Elastic	2	0.3357
0.3	Elastic	4	0.50972
0.3	Elastic	7	0.76393
0.3	Elastic	9	0.92628
0.3	Elastic	10	1.0047
0.3	Elastic	11	1.08102
0.3	Elastic	13	1.2267
0.3	Elastic	15	1.36205
0.3	Elastic	17	1.48604
0.3	Elastic	20	1.64899

MACH	Rigidity	ALPHA	CL
0.3	Rigid	0	0.17148
0.3	Rigid	2	0.35714
0.3	Rigid	4	0.541
0.3	Rigid	7	0.80886
0.3	Rigid	9	0.97924
0.3	Rigid	10	1.06129
0.3	Rigid	11	1.14096
0.3	Rigid	13	1.29246
0.3	Rigid	15	1.4324
0.3	Rigid	17	1.55972
0.3	Rigid	20	1.7254

% DIFFERENCE
-6.570952053
-6.00301845
-5.78332138
-5.554497823
-5.408082611
-5.332190071
-5.253470761
-5.087971775
-4.911337615
-4.723924807
-4.42853831

Figure 3.4 : Elastic Shape - Rigid Shape, Mach: 0.3.

As shown in Figures 3, 4, and 3.5, the losses due to elastic effects are significant and cannot be underestimated in aircraft. In aircraft design, these graphs provide important evidence for considering elastic effects.

MACH :0.6

MACH	Rigidity	ALPHA	CL
0.6	Elastic	0	0.18214
0.6	Elastic	2	0.37984
0.6	Elastic	4	0.57243
0.6	Elastic	7	0.83955
0.6	Elastic	9	0.9964
0.6	Elastic	10	1.06718
0.6	Elastic	11	1.13251
0.6	Elastic	13	1.24644
0.6	Elastic	15	1.33856
0.6	Elastic	17	1.41097
0.6	Elastic	20	1.49101

MACH	Rigidity	ALPHA	CL
0.6	Rigid	0	0.19715
0.6	Rigid	2	0.4081
0.6	Rigid	4	0.61257
0.6	Rigid	7	0.89322
0.6	Rigid	9	1.05558
0.6	Rigid	10	1.12805
0.6	Rigid	11	1.19443
0.6	Rigid	13	1.30877
0.6	Rigid	15	1.39965
0.6	Rigid	17	1.47
0.6	Rigid	20	1.54703

% DIFFERENCE
-7.613999493
-6.923125931
-6.553036301
-6.008045059
-5.606396483
-5.39603741
-5.184062691
-4.762486915
-4.364662594
-4.015646259
-3.621132105

Figure 3.5 : Elastic shape - Rigid shape, Mach: 0.6.

MACH :0.9

MACH	Rigidity	ALPHA	CL
0.9	Elastic	0	0.26431
0.9	Elastic	2	0.54456
0.9	Elastic	4	0.80504
0.9	Elastic	7	1.12104
0.9	Elastic	9	1.26906
0.9	Elastic	10	1.3251
0.9	Elastic	11	1.36841
0.9	Elastic	13	1.43357
0.9	Elastic	15	1.48482
0.9	Elastic	17	1.52507
0.9	Elastic	20	1.58451

MACH	Rigidity	ALPHA	CL
0.9	Rigid	0	0.30068
0.9	Rigid	2	0.60973
0.9	Rigid	4	0.88925
0.9	Rigid	7	1.21101
0.9	Rigid	9	1.352
0.9	Rigid	10	1.40338
0.9	Rigid	11	1.44488
0.9	Rigid	13	1.50667
0.9	Rigid	15	1.55147
0.9	Rigid	17	1.58947
0.9	Rigid	20	1.64144

% DIFFERENCE
-12.09429325
-10.68861288
-9.469858409
-7.429335844
-6.134615385
-5.577961778
-5.292481036
-4.851759178
-4.295925799
-4.05166502
-3.46829613

Figure 3.6 : Elastic shape - Rigid shape, Mach: 0.9.

The lift coefficient values for the elastic (flight shape) and rigid shape of the RQ-4 Global Hawk aircraft at Mach 0.3, Mach 0.6, and Mach 0.9 are shown in the Figures 3.4, 3.5, 3.6; respectively. When looking closely at the tables, aerodynamic losses due to angle of attack are observed for all Mach number values.

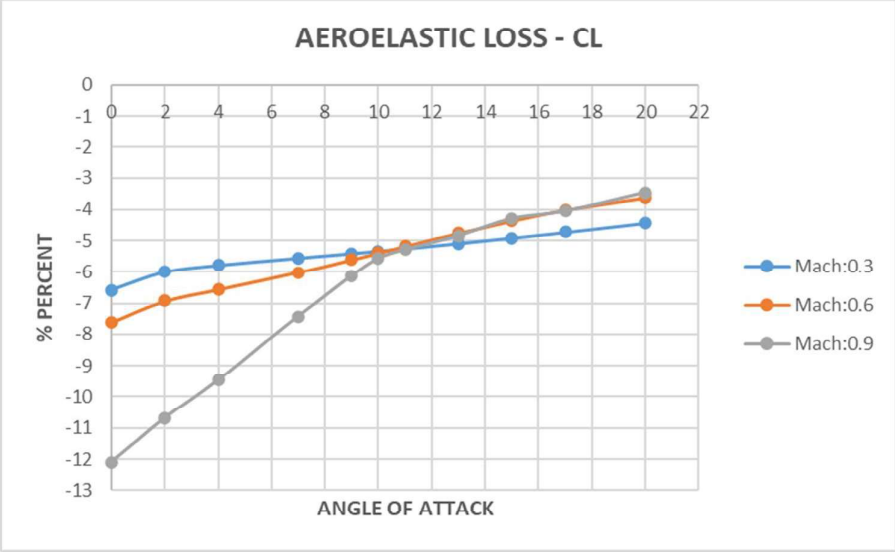

Figure 3.7 : Aeroelastic loss in terms of lift coefficient.

To better illustrate the loss due to aeroelastic effects, all aeroelastic loss tables are overlaid in Figure 3.7. It is observed that aeroelastic loss is higher at lower angles of attack. Upon careful analysis of Figure 3.7, it is estimated that the loss due to aeroelastic effects is bigger than 3.5% for all Mach number values.

Due to its high aspect ratio wing design, the RQ-4 Global Hawk aircraft experiences pronounced aeroelastic effects to keep its weight light and not compromise its range. Aeroelastic effects are particularly noticeable in the decrease of lift coefficient, while relatively, the drag coefficient and induced drag coefficient values do not change

significantly due to elastic effects. Consequently, when calculating the lift-to-drag ratio, a simple performance parameter, the performance value of the RQ-4 Global Hawk aircraft decreases.

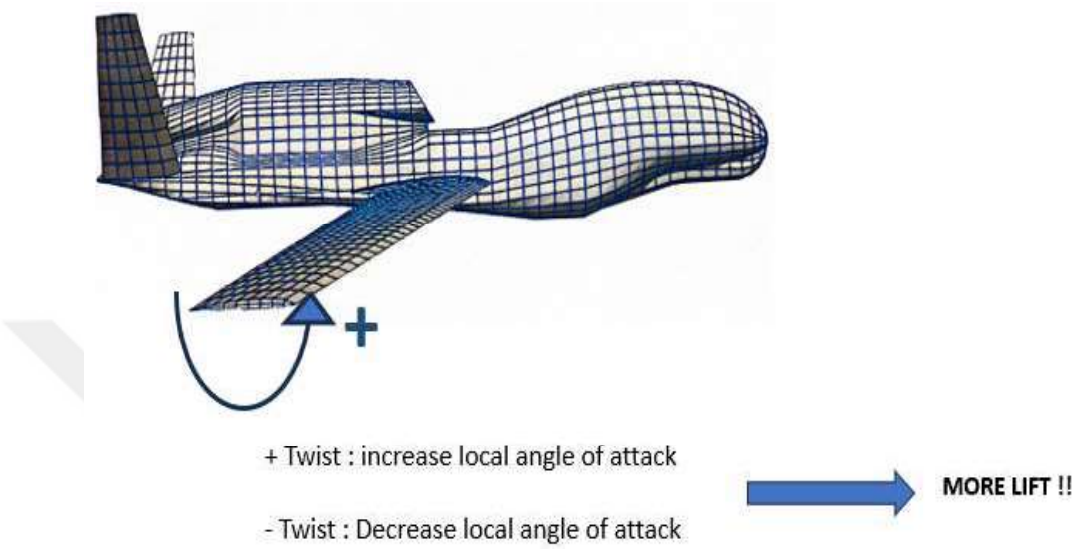

Figure 3.8 : ZONAIR twist sign convention.

When defining the jig shape, as mentioned in section 3.2, the downward twist of the wing's airfoil reduces the aerodynamic coefficient value. To verify this, the flight shape analysis examines whether the airfoils have a twist up or down. Figure 3.8 illustrates whether the RQ-4 Global Hawk aircraft's ZONAIR model has twist + or -, indicating twist up or twist down.

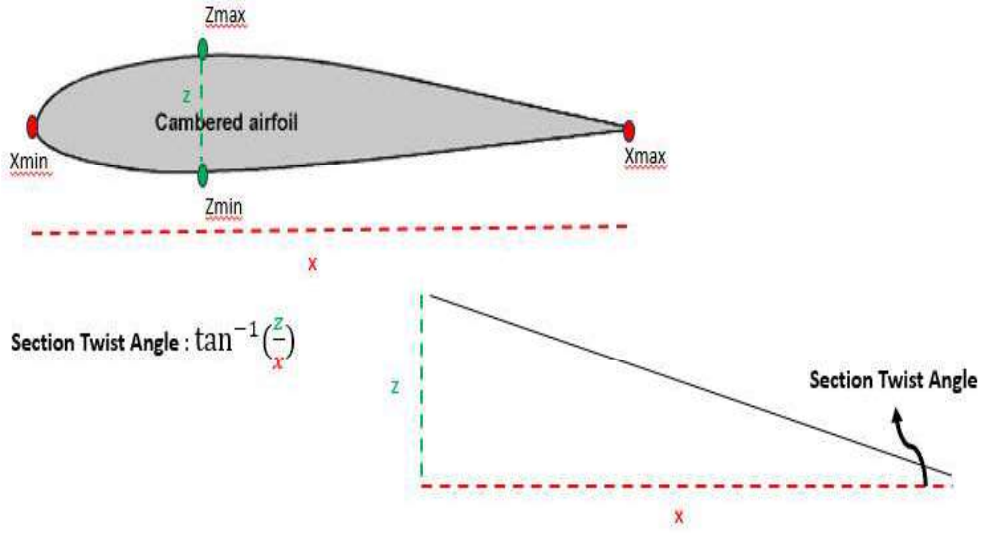

Figure 3.9 : Section twist calculation.

Each airfoil section's twist angle is calculated as shown in Figure 3.9. The direction from the leading edge to the trailing edge is critical in determining whether it's Twist Up or Down.

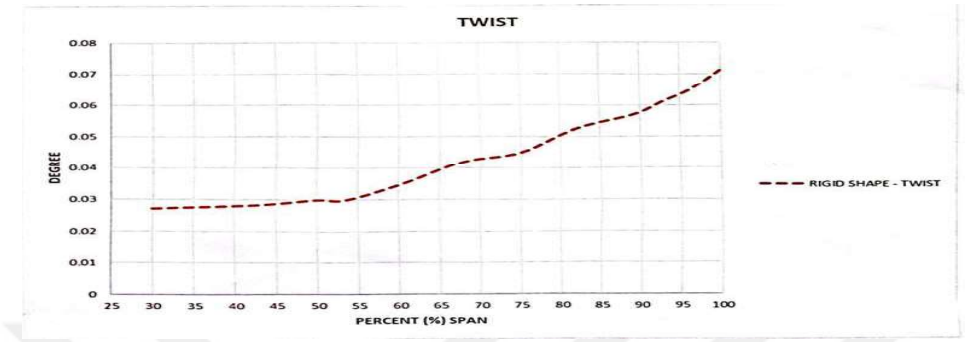

Figure 3.10 : Section twist, Mach: 0.6, AoA: 6 degree, Rigid aicraft.

Figure 3.10 shows the measured twist value of the rigid aircraft from spanwise root to tip.

Figure 3.11 : Section twist, Mach: 0.6, AoA: 6 degree, Elastic aicraft.

In Figure 3.11, the section twists of the rigid and elastic aircraft are shown. Mach 0.6 and an angle of attack of 6 degrees was selected as an example case. When the flight shape is calculated using ZONAIR, a decrease in the lift coefficient is observed due to elastic effects. The twist down of the section twists decreases the lift coefficient value. Upon detailed examination of Figure 3.11, it can be seen that for this example case, the airfoil sections are twisted down, resulting in a decrease in the lift coefficient value.

This result highlights why it's important to include elastic effects in aerodynamic modeling. The twist in the airfoil sections decreases the lift coefficient and shows how these deformations impact performance. By considering these effects, engineers can make better design choices and improve the aircraft's efficiency. This helps ensure that the design meets performance requirements under different flight conditions.

4. METHODOLOGY

Calculating the jig shape is an iterative process. Therefore, the calculation of the jig shape needs to be done according to a specific logic.

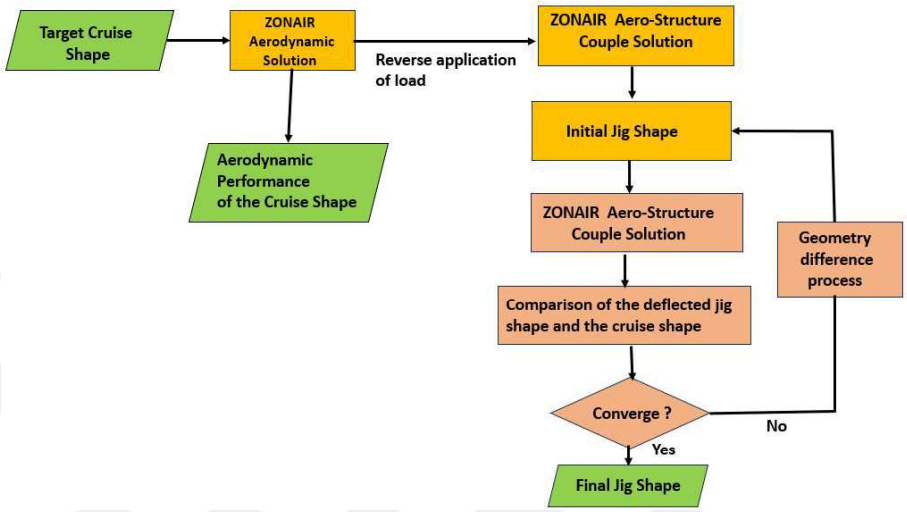

Figure 4.1 : Jig shape calculation flowchart.

The flowchart for calculating the jig shape is shown in Figure 4.1. According to this flowchart, the aerodynamic performance of the aerodynamically optimized wing is measured, and based on that performance, the aircraft's mission is selected. However, when an aerodynamically optimized wing is produced, it flexes and deforms due to elastic effects. In this case, estimated values of aircraft, falls below the target performance values. Therefore, the jig shape calculation is performed to design the aircraft.

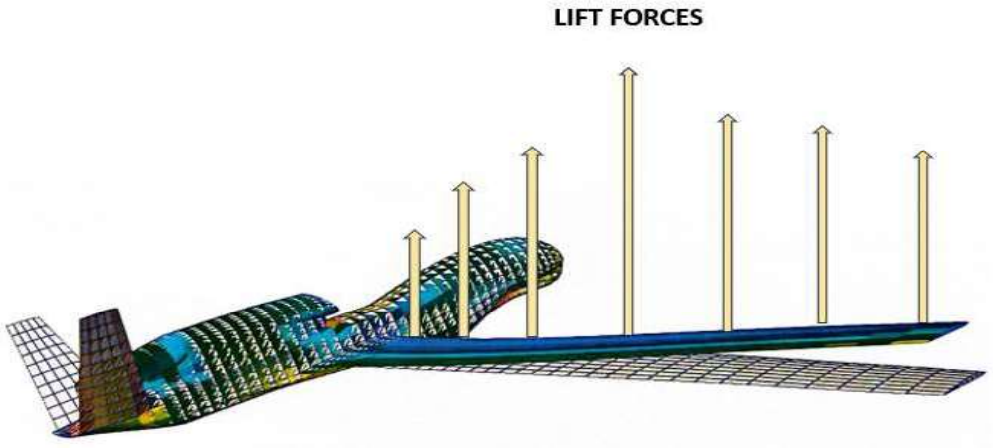

Figure 4.2 : Mach:0.6, AoA: 6 degree, Flight Shape.

In this study, the calculation of the jig shape will be conducted using the ZONAIR solver. Upon detailed examination of Figure 4.2, the optimized state of the RQ-4 Global Hawk aircraft is represented by the geometry with a meshed outer surface. The flight shape, on the other hand, is depicted as the deformed contoured shape. Aerodynamic analysis is performed using the ZONAIR aerodynamic solver to extract aerodynamic loads. A comparison is made between the aerodynamic performance of the rigid shape and the performance of the elastic (flight) shape. Figure 4.1 illustrates the rigid and elastic (flight) shapes of the RQ-4 Global Hawk aircraft.

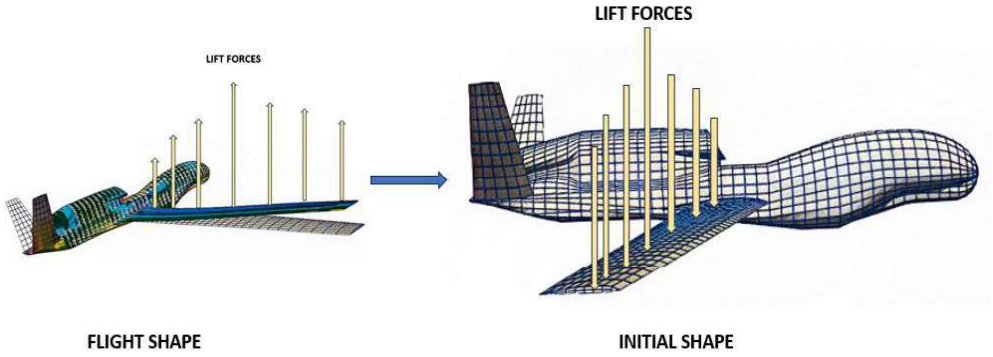

Figure 4.3 : Reverse Application of Load.

After extracting the aerodynamic loads of the RQ-4 Global Hawk aircraft, a ZONAIR aerostructural solution is obtained by multiplying the same loads by minus one, effectively changing their direction, and applying them to the aerodynamically optimized aircraft. This process can be thought of as similar to a one-way Fluid-Structure Interaction (FSI). Using the equation sets mentioned in ZONAIR 3.2 section, rigid aerodynamic loads are determined and then applied in reverse to the aircraft by inverting these loads. Figure 4.3 illustrates this process.

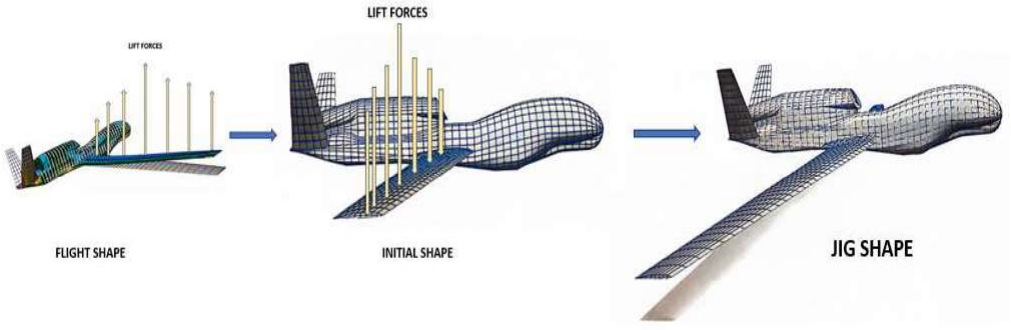

Figure 4.4 : Jig shape results.

Figure 4.4 shows that the inverted aerodynamic loads, applied to the initial shape, resulting in the initial jig shape through aerostructural analysis in ZONAIR. This initial shape, which is the jig shape, is obtained following the flowchart shown in Figure 4.1 using ZONAIR. Subsequently, an aero-structural analysis is performed in ZONAIR using the obtained jig shape. The aerodynamic performance of the targeted cruise shape is compared with the aero-structural solution of the initial jig shape (i.e., the flight shape resulting from the first iteration) in Figure 4.1.

The aerostructural solution is obtained using the ZONAIR solver. Since the aim of this thesis is to accelerate the jig shape calculation process, the ZONAIR solver is utilized. Traditional methods require the setup of highly complex models for jig shape calculation, and the solutions for these models take a long time to compute. This is because the transition from rigid shape to flight shape is achieved through Fluid-Structure Interaction (FSI), followed by transitioning to the jig shape based on this flight shape calculation. Due to these complexities, traditional methods are not commonly integrated into aircraft design processes. However, designing aircraft with jig shape calculations during the design process results in aircraft designs that closely approximate the targeted aircraft performance.

5. JIG SHAPE OPTIMIZATION

Since the jig shape calculation is a long iterative process, the final jig shape can be found by trying numerous combinations of variables. Given the many possible combinations for the wing, this process should be performed according to a specific logic and constraints. Using a defined optimization method makes this process more efficient and effective. As shown in Figure 5.1, the iterations will continue until the desired objective function is achieved.

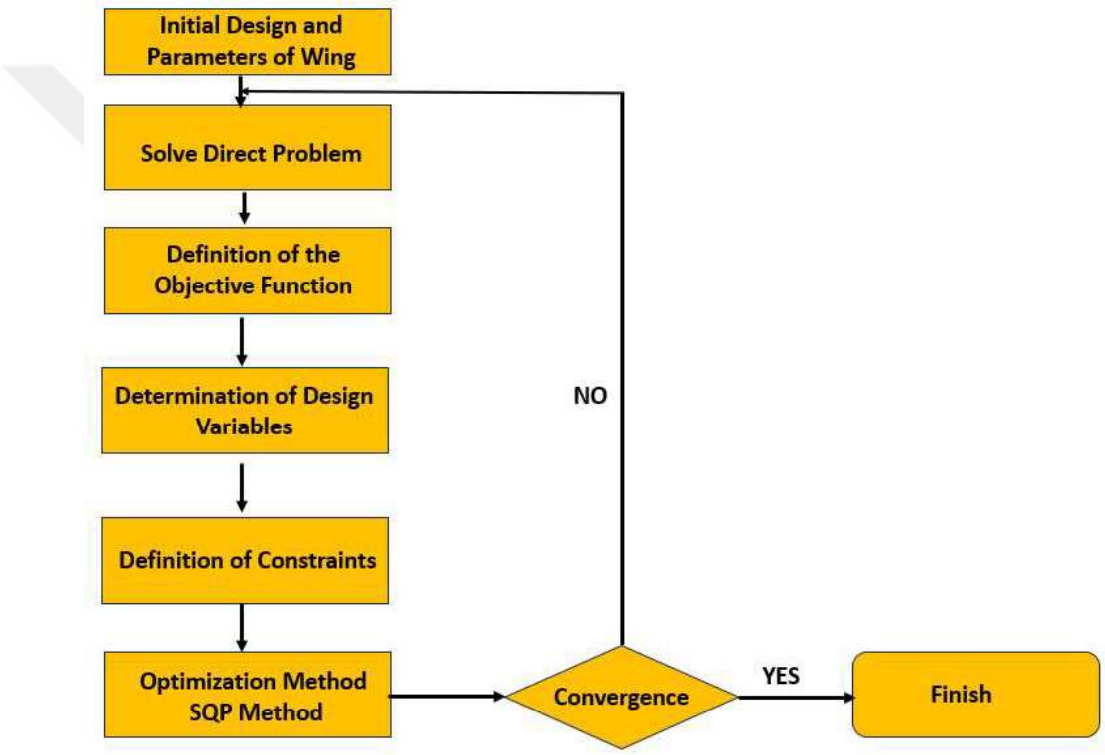

Figure 5.1 : Jig Shape optimization flowchart.

There are many optimization methods and techniques. The optimization method should be chosen based on the optimization problem.

There are two kinds of optimization methods in principle:

- Mathematical programming methods (Deterministic and analytical methods)
  - Unconstrained Methods
    - Steepest Descent
    - Conjugate Gradient

        - Quasi-Newton
        - Newton
    - Constrained Methods
        - Linear Simplex
        - SLP (Linear)
        - SQP (Nonlinear)
        - Exterior Penalty(Nonlinear)
        - Interior Penalty (Nonlinear)
        - GRC (Nonlinear)
        - MFD (Nonlinear)
        - Mixed Integer Programing
- Mathematical programming methods (Deterministic and analytical methods)
    - Nelder- Mead Simplex (Nonlinear Simplex)
    - Simulated Annealing
    - Divided Rectangles Method
    - Genetic Algorithms
    - Particle Swarm Optimization

When choosing an optimization method, the following criteria should be considered: whether the final design is realistic, confidence in convergence, computational cost, and whether additional boundary conditions are needed as iterations progress [18]. Considering these questions helps in selecting the appropriate optimization method. In this study, the Sequential Quadratic Programming (SQP) method has been selected.

5.1 Sequential Quadratic Programming (SQP)

Sequential Quadratic Programming (SQP) is an optimization method that solves a sequence of quadratic subproblems to find the optimal solution. It is especially effective for problems with nonlinear objective functions and constraints.

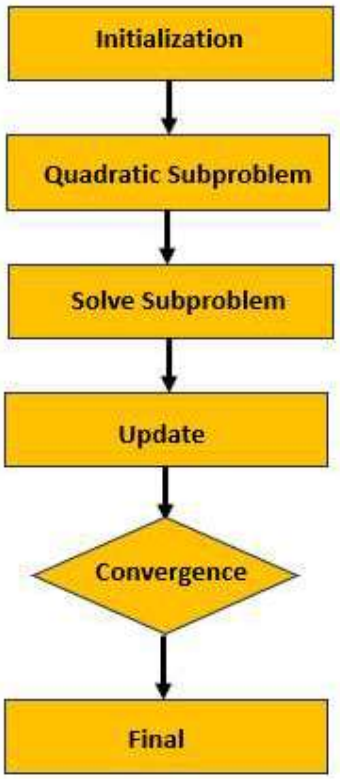

Figure 5.2 : Sequential quadratic programming.

Sequential Quadratic Programming (SQP) method can be explained in five steps which is shown in Figure 5.2. The SQP method starts with an initial guess for the design variables. In each iteration, a quadratic approximation of the objective function is created. This means expressing the original nonlinear problem approximately with a simpler quadratic problem. Constraints are linearized around the current guess. Then, a search direction is found by solving the quadratic subproblem. This step aims to minimize the quadratic approximation and satisfy the linearized constraints. After each iteration, progress is made from the current guess in the direction found [17]. If it seems like convergence is not achievable based on the results, the design variables are updated to this new position. After convergence check, if convergence is achieved, the optimization is terminated; otherwise, the process continues with the new design variables [19].

SQP method has several advantages. It improves the solution iteratively, ensuring high accuracy. It aims to efficiently solve problems by converting constraints into linear approximations. Additionally, it can handle a wide range of constraints, both linear and nonlinear, leading to effective solutions. SQP method is utilized when the

objective function and constraints of an optimization problem are nonlinear, requiring high precision in the solution, and when the problem size is small to moderate.

Sequential Quadratic Programming (SQP) algorithm can be explained in a simpler way. The first step is to choose an initial point, which is used in this initial guess. At the starting point, the QP subproblem is formulated. This QP subproblem is created by using a quadratic approximation of the objective function and linearizing the constraints.

$$x_0: \text{initial guess} \tag{5.1}$$

$$f(x_k) + \nabla f(x_k)^T d + \frac{1}{2} d^T \nabla^2 f(x_k) d \tag{5.2}$$

$$x_{k+1} = x_k + d \tag{5.3}$$

$$g_i|(x_{k+1}) = g_i|(x_k) + \nabla g_i(x_k) + \nabla g_i(x_k)^T d = 0, i = 1,2.. \tag{5.4}$$

The search direction d is found by solving the QP subproblem. In this step, the best search direction is calculated using a QP solver. The design variables are updated using the found search direction.

$$x_{k+1} = x_k + d \tag{5.5}$$

The new design variables $\boldsymbol{x_{k+1}}$ are then checked to see if they meet the desired accuracy or convergence criteria. For example, a change criterion such as $\boldsymbol{f(x_{k+1}) - f(x_k)}$ or $\boldsymbol{|x_{k+1} - x_k|}$ can be used. If the criterion is not met, the steps are repeated.

In this study, the Sequential Quadratic Programming (SQP) method was employed. The first step in setting up the optimization problem is to find a method that can modify the x, y, and z points of each grid to be modified. To morph the mesh on the surface, the Laplacian Mesh Editing method will be used. The basic formulas and mathematical expressions of Laplacian Mesh Editing allow for natural and realistic deformations according to user-defined constraints while preserving local geometry in mesh deformation operations. The SQP method is applied using the search direction from Equation (5.5) based on Equation (5.4). As a result of the optimization, the outer surface is updated according to the optimized values with the help of PyPAD.

The PyPAD library, which contains the Laplacian Mesh Editing method, is used in Python to easily morph these points. The equations underlying Laplacian Mesh Editing in the PyPAD library are as follows.

$$\mathrm{L}vi^{x} = \sum j \in N(i)(vj^{x} - vi^{x}) \quad (5.6)$$

$$\mathrm{L}vi^{y} = \sum j \in N(i)(vj^{y} - vi^{y}) \quad (5.7)$$

$$\mathrm{L}vi^{z} = \sum j \in N(i)(vj^{z} - vi^{z}) \quad (5.7)$$

The Laplacian operator is calculated separately for each node's x, y, and z coordinates. 〖vi〗 ^x, 〖vi〗 ^y, 〖vi〗 ^z represent the x, y, and z coordinates of node i, respectively. N(i): Neighbors of node *i*i, which is node number *i*.

$$\delta_{\mathrm{i}}{}^{\mathrm{x}} = \mathrm{Lv_i}{}^{\mathrm{x}} \quad (5.9)$$

$$\delta_{\mathrm{i}}{}^{\mathrm{y}} = \mathrm{Lv_i}{}^{\mathrm{y}} \quad (5.10)$$

$$\delta_{\mathrm{i}}{}^{\mathrm{z}} = \mathrm{Lv_i}{}^{\mathrm{z}} \quad (5.11)$$

Differential coordinates are calculated separately for each node's x, y, and z coordinates.

$$\mathrm{minV'x} \parallel \mathrm{LV'}^{\mathrm{x}} - \delta^{\mathrm{x}} \parallel^{2} \quad (5.12)$$

$$\mathrm{minV'y} \parallel \mathrm{LV'}^{\mathrm{y}} - \delta^{\mathrm{y}} \parallel^{2} \quad (5.13)$$

$$\mathrm{minV'z} \parallel \mathrm{LV'}^{\mathrm{z}} - \delta^{\mathrm{z}} \parallel^{2} \quad (5.14)$$

The optimization problem is formulated separately for each coordinate. The goal is to find the new x, y, and z positions of the nodes while preserving the differential coordinates. The new node positions are represented as shown above, along with the original differential coordinates. Using the equation sets from (5.12), (5.13) and (5.14) a surface will be created where each variable's coordinates are realistic and exhibit smooth transitions. In optimization problems, having a non-complex equation contributes to the problem being well-defined. Therefore, the equation sets used to determine the coordinates of the variables have been chosen to be simple.

subject to $Vi'^{x} = vi^{x}$ for all constrained vertices

subject to $Vi'^{y} = vi^{y}$ for all constrained vertices

subject to $Vi'^{z} = vi^{z}$ for all constrained vertices

The optimization problem is solved by adding constraints to the positions of specific node points.

$$L^{T}LV'^{x} = L^{T}\delta^{x} \tag{5.15}$$

$$L^{T}LV'^{y} = L^{T}\delta^{y} \tag{5.16}$$

$$L^{T}LV'^{z} = L^{T}\delta^{z} \tag{5.17}$$

The nodes of the mesh that will be morphed are modified using a linear system solution. In the PyPAD library, this is done using sets of equations.

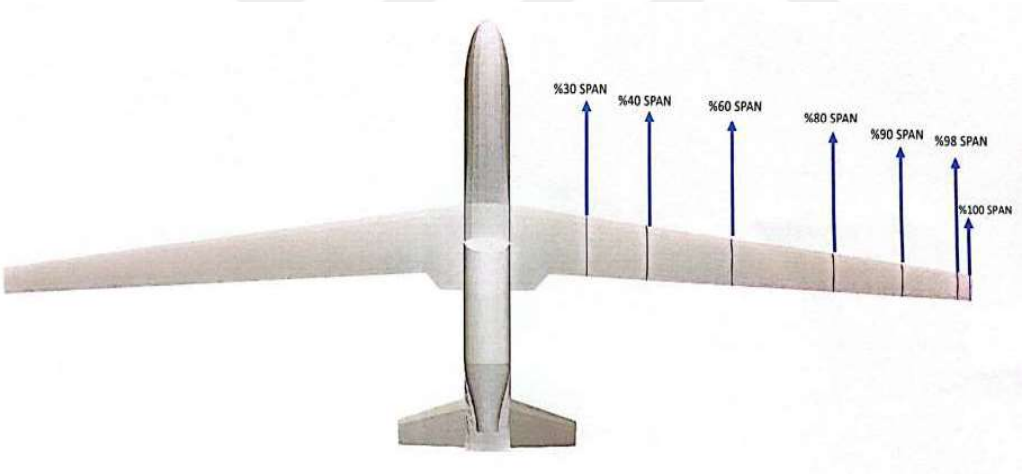

Figure 5.3 : Design Airfoil Sections.

In light of this information, the parametrized profiles of the wing for jig shape optimization of the RQ-4 Global Hawk aircraft have been determined which is shown in Figure 5.3. If an optimization model for the RQ-4 Global Hawk aircraft is to be established, the first task should be to define the design variables. For the RQ-4 Global Hawk aircraft, a total of 6 sections are selected as design variables. These 6 sections include 6 twist angles, 6 dihedral angles, and the wing area of the RQ-4 Global Hawk aircraft as a design variable.

The design variables are as follows:

Twist angle: $\theta_1,\ \theta_2,\ \theta_3\ ,\theta_4,\ \theta_5,\ \theta_6$

Section displacement: $\Gamma_1,\ \Gamma_2,\ \Gamma_3,\ \Gamma_4,\ \Gamma_5,\ \Gamma_6$

Wing Area: S_{wing}

In the jig shape optimization model of the RQ-4 Global Hawk aircraft, the objective function is to match the aircraft's shape during flight with the target shape. When setting up the mathematical model of this optimization problem, Python's PyPAD library is used to approach the x, y, and z points of the aircraft's specified seven sections to the x, y, and z points of the target shape.

In jig shape optimization, setting up the mathematical model should be done carefully and accurately. This is because choosing the wrong parameters can lead the optimization in the wrong direction. Since the optimization technique is gradient-based, If the objective function is minimized, there's a risk of reaching a local minimum rather than the global minimum, potentially causing confusion about the intended goal of finding the global minimum point. The optimization model in this optimization problem is built based on the method of minimizing the objective function.

The objective function is represented as follows:

$$\text{Minimize } \sum_i ((x_i{}^{hedef} - xi)^2 + (y_i{}^{hedef} - yi)^2 + (z_i{}^{hedef} - zi)^2) \qquad (5.18)$$

This function sums the squares of the differences between each profile point and the target profile. Minimizing this value indicates that the wing is closer to the target profile. If the result of this function is close to zero, then it shows that the wing's actual profile closely matches the target profile.

The optimization process for the RQ-4 Global Hawk aircraft will utilize the Sequential Quadratic Programming (SQP) method, which is a gradient-based optimization technique. This method has shown considerable success in problems of moderate or smaller scale. It's crucial to direct the optimization during the setup of the mathematical model, meaning that the mathematical model needs to be well-defined. For the optimization model to be well-defined, it's crucial to have a comprehensive set of constraints in the mathematical model.

During the modeling of the optimization, the fuselage and vertical tail of the aircraft are initially kept fixed, meaning their external geometries remain unchanged. Only 6 sections on the wings are used for the optimization process. The most critical aspect being considered in these 6 sections is to maintain the external geometry realistically and avoid introducing sweep angles to the aircraft's wing. Therefore, after each optimization, it is ensured that the design variables remain in a realistic form.

The constraints are as follows:

$$55\ m^2 < S_{wing\ area} < 57\ m^2 \tag{5.19}$$

$$\text{Section displacement : } \Gamma_1 < \Gamma_2 < \Gamma_3 < \Gamma_4 < \Gamma_5 < \Gamma_6 \tag{5.20}$$

$$\text{Twist angle: } \theta_1 < \theta_2 < \theta_3 < \theta_4 < \theta_5 < \theta_6 \tag{5.21}$$

$$C_{root} = \text{Constant} = 2.847\ m \tag{5.22}$$

$$C_{tip} = \text{Constant} = 0.823\ m \tag{5.23}$$

$$-2\ \text{degree} < \theta_1, \theta_2, \theta_3, \theta_4, \theta_5, \theta_6 < +2\ \text{degree} \tag{5.24}$$

$$-1.5\ m < \Gamma_1, \Gamma_2, \Gamma_3, \Gamma_4, \Gamma_5, \Gamma_6 < 1.5\ m \tag{5.25}$$

The math model for jig shape optimization is defined above. Essential elements like the objective function, constraints, and design variables are specified in an optimization model. The constructed optimization model is compact and well-defined. The goal of this study is to shorten the jig shape optimization process. In this study, jig shape calculation involves changing only the outer mold lines on the wings without altering the structural layout.

In the optimization model, the variables demonstrate the following: Equation (5.19) indicates that the wing area can vary within a specified range, while Equation (5.20) shows that the dihedral angle changes according to specific sectional locations. Equation (5.21) represents the twist angle of the wing. Additionally, Equation (5.22) specifies that the root of the wing has a fixed value, and Equation (5.23) confirms that the tip chord of the wing is also set at a constant value.

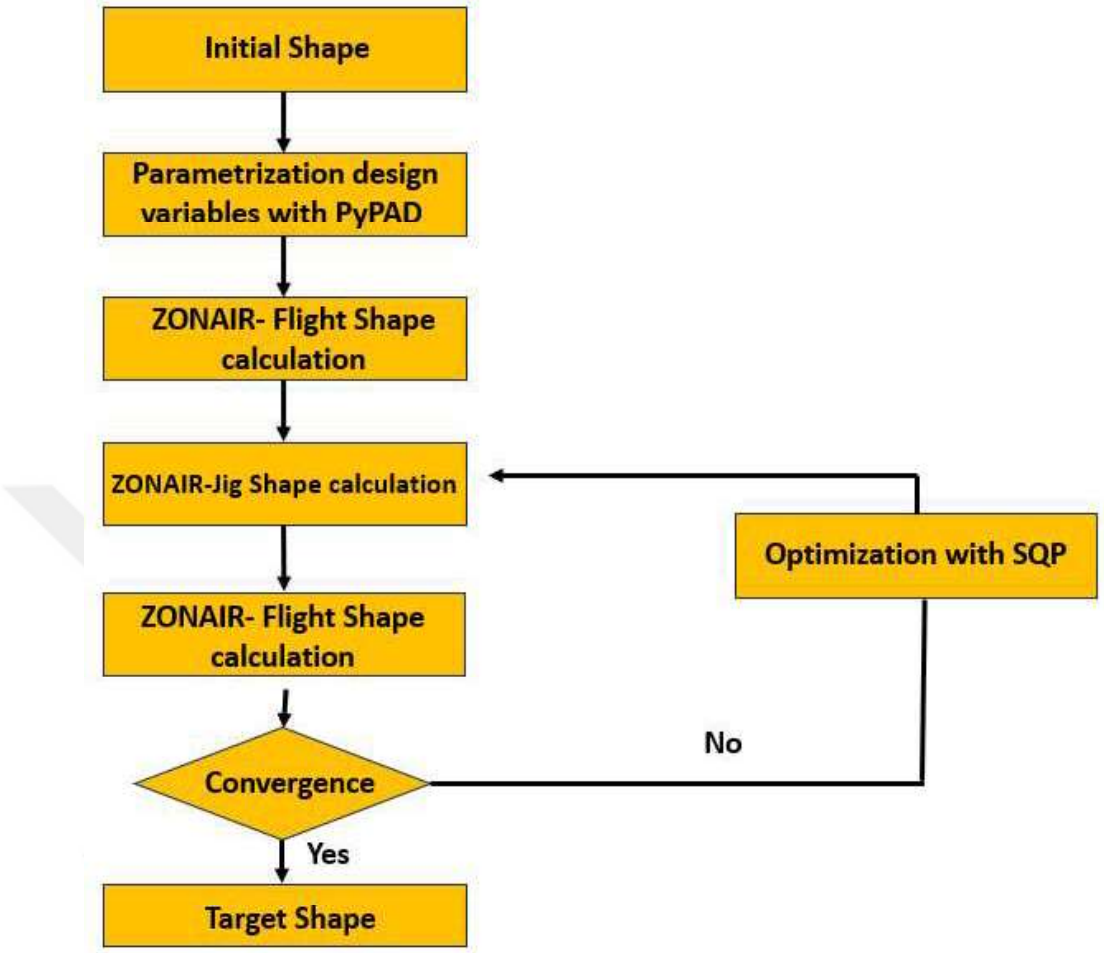

Figure 5.4 : Jig shape optimization process.

In this study, ZONAIR and Python were integrated to communicate with each other, thereby automating the jig shape optimization process. Firstly, the design variables of the aerodynamically optimized target shape, i.e., cruise shape geometry, are parameterized using Python's PyPAD library. Then, they are sent to the ZONAIR solver, which calculates the aircraft's flight shape. The calculated flight shape is sent to the ZONAIR solver through Python code, and through this solver, the first iteration of jig shape is calculated. This shape is subsequently sent to the ZONAIR solver for solving, and the flight shape is calculated which is shown in Figure 5.4.

The calculated flight shape is compared geometrically with the target shape to determine how much difference exists, and whether this difference is below the specified limit is checked. If it's below the specified limit, the optimization is considered to be converged. However, if it exceeds the specified limit, a second iteration is initiated by providing new inputs to the parameterized variables using

Python code and the PyPAD library, and then subjected to SQP optimization. After the optimization with SQP, the second iteration's second jig shape is found and sent to ZONAIR. Through the ZONAIR solver, the flight shape is calculated and compared with the target shape. This optimization process continues until the specified convergence limit is reached.

Table 5.1 : Optimization design variable.

Design Variable	Initial Value	Optimized Value
θ_1	+0.0013 degree	+0.2956 degree
θ_2	+0.0048 degree	+0.3128 degree
θ_3	+0.0066 degree	+0.4325 degree
θ_4	+0.0087 degree	+0.6248 degree
θ_5	+0.0165 degree	+0.7442 degree
θ_6	+0.0189 degree	+0.8126 degree
$\Gamma_{1,}$	0 meter	0.0856 meter
$\Gamma_{2,}$	0 meter	0.1223 meter
$\Gamma_{3,}$	0 meter	0.2489 meter
$\Gamma_{4,}$	0 meter	0.3625 meter
$\Gamma_{5,}$	0 meter	0.4234 meter
$\Gamma_{6,}$	0 meter	0.4886 meter
$S_{wing\ area}$	56.14 m^2	56.8876 m^2

The optimization process has ended as the limit set for the objective function has been reached. In total, it took 11 iterations for the objective function to converge to the specified limit. Table 5.1 provides the initial values of the design variables and the final values of the jig shape model. When questioned if the optimized values are realistic, these values are found to be realistic and reasonable.

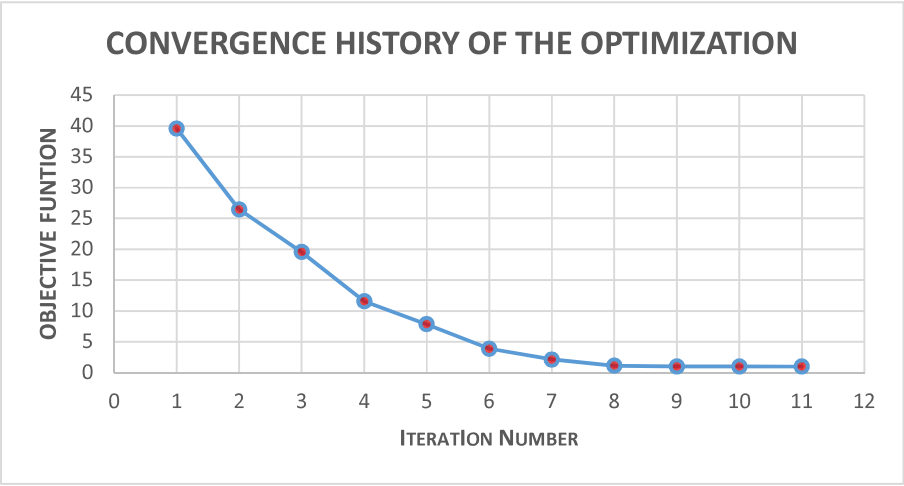

Figure 5.5 : Convergence history of the optimization.

The optimization has been completed as the convergence history shows that the objective function has dropped below the threshold value set. As can be seen in Figure 5.5, an optimal solution was achieved after 11 iterations. The optimization algorithm is written in Python, and since the size of the problem to be optimized is small, the solution time is incredibly fast. Each solution by ZONAIR takes approximately 48 seconds, and preparing the optimization code for the next iteration takes 35 seconds. Each iteration takes less than 2 minutes.

The optimization process turned out to be much faster than anticipated. Each iteration took less than 2 minutes, including approximately 48 seconds for ZONAIR to solve the problem and 35 seconds to prepare the optimization code for the next iteration. This swift progress was made possible by the small size of the problem and the efficient optimization algorithm written in Python.

As shown in Figure 5.5, a solution was reached in just 11 iterations. During these iterations, the objective function dropped below the set threshold, indicating the successful completion of the optimization. This fast and efficient process significantly contributed to the overall project timeline, allowing us to reach the desired results much sooner than expected.

If the results of the last three iterations for target, flight, and jig shape are to be shown,

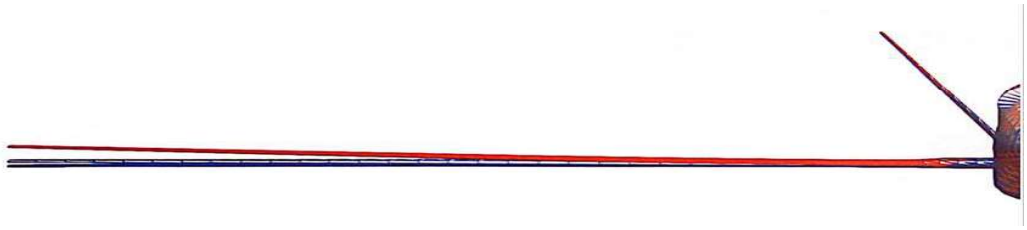

Figure 5.6 : 9th iteration.

Figure 5.6 displays the 9th iteration. The red color represents the flight shape, the blue color represents the jig shape, and the mesh-like gray color represents the target shape.

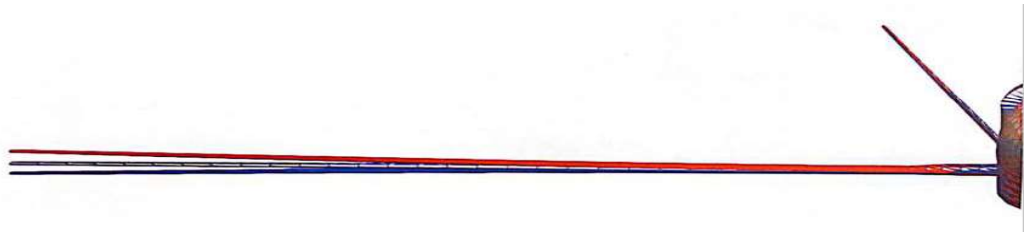

Figure 5.7 : 10th iteration.

Figure 5.7 displays the 9th iteration. The red color represents the flight shape, the blue color represents the jig shape, and the mesh-like gray color represents the target shape (i.e., cruise shape).

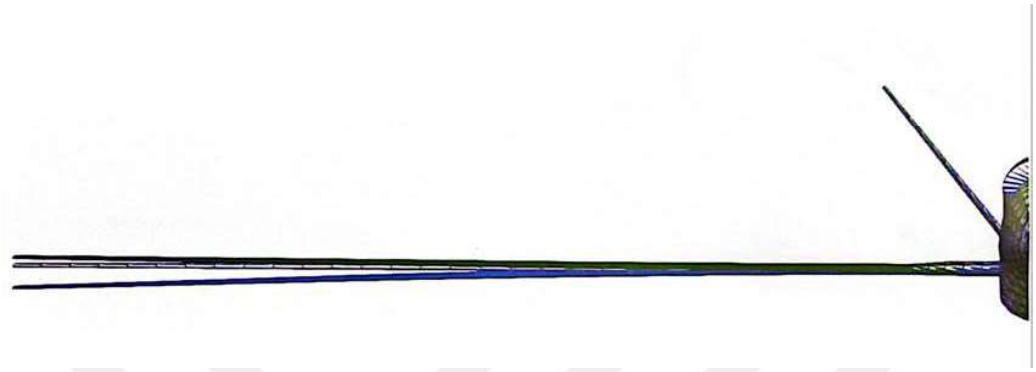

Figure 5.8 : 11 th Iteration.

Figure 5.8 displays the 9th iteration. The green color represents the flight shape, the blue color represents the jig shape, and the mesh-like gray color represents the target shape (i.e., cruise shape).

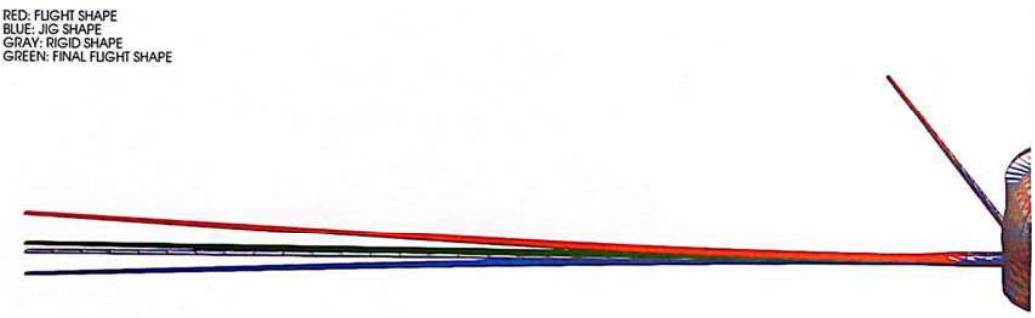

Figure 5.9 : Initial flight shape and jig shape optimized shape.

As seen in Figure 5.9, when we directly fly the initial aircraft under aeroelastic effects, it will deviate from the target shape due to elastic influences. However, it is possible to reach the desired target shape by performing jig shape optimization. Jig shape optimization can make the aircraft more efficient. In Figure 5.9, the red color represents the initial flight shape, while the green color represents the flight shape after jig shape optimization. Upon closer inspection, it can be seen that the target shape is very close. Upon closer examination of the results from the 11th iteration, the twist and dihedral values are plotted in Figure 5.10.

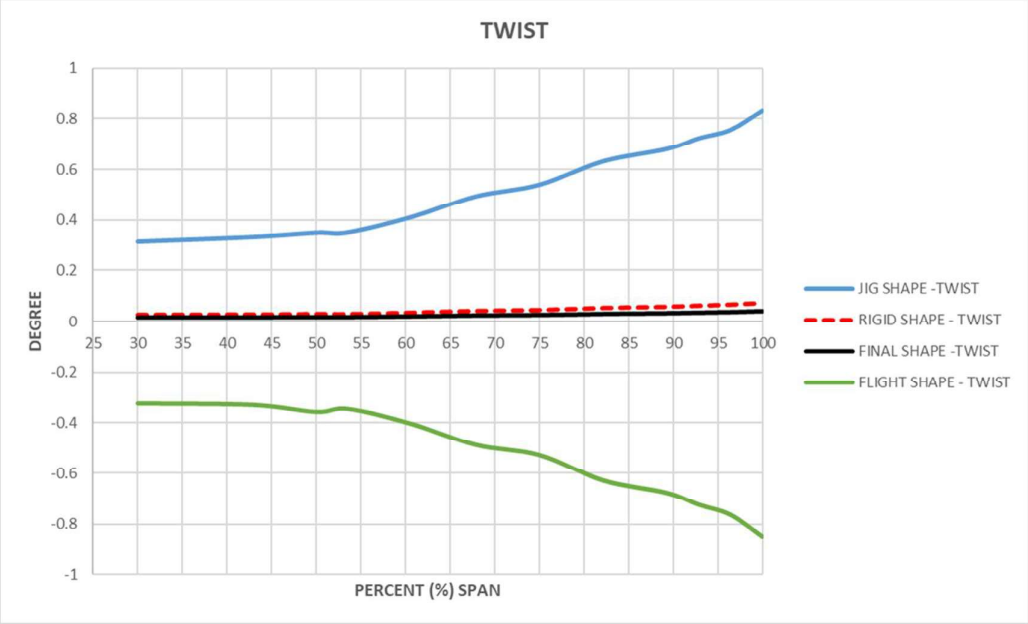

Figure 5.10 : The twist distribution of wing on 11th iteration.

Figure 5.10 depicts the twist distribution across sections on the wing after the 11th iteration. The optimized twist values are within the constraints. Upon examining operational aircraft, this optimized twist value is realistic and represents a relatively low twist value.

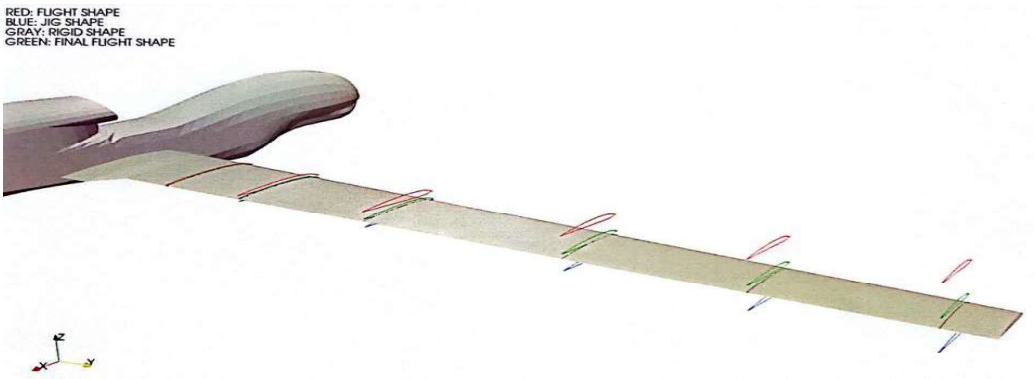

Figure 5.11 : Displacement of wing.

Figure 5.11 displays the displacements across sections on the wing after the 11th iteration. The optimized displacement values are within the constraints. Upon examining operational aircraft, these optimized displacement values are realistic and consistent with observed values in practice.

The lift coefficient-angle of attack curve of the initial flight shape and the results obtained in the last three iterations for Mach 0.3, 0.6 and 0.9 respectively are shown in Figure 5.12, 5.13, and 5.13.

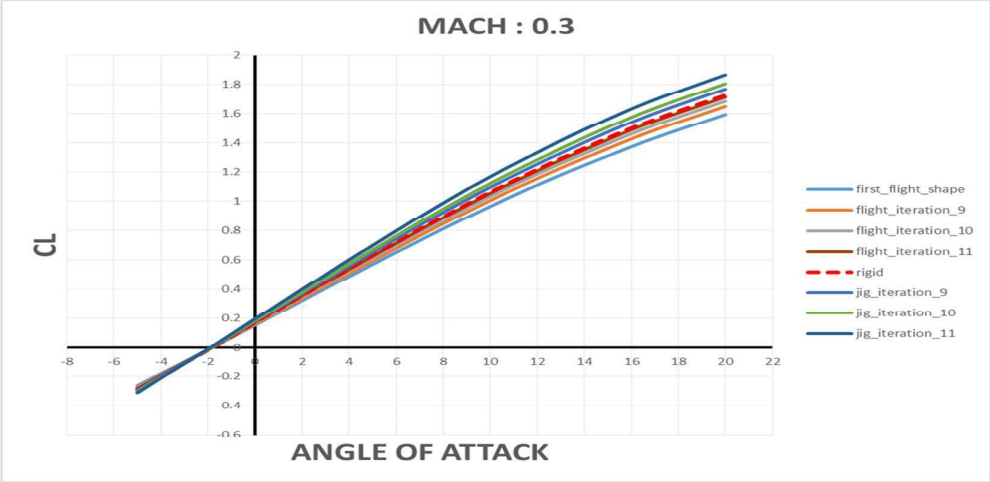

Figure 5.12 : Last 3 iteration, Mach: 0.3.

After the optimization model is established, the model is executed. The RQ-4 Global Hawk aircraft is optimized. The optimization achieved after 11 iterations. The results of the last three iterations are shown.

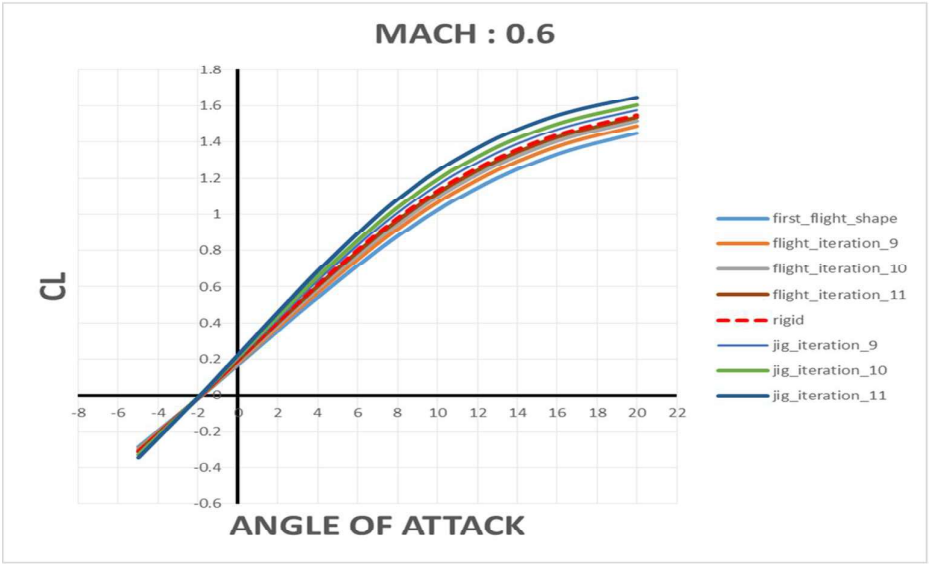

Figure 5.13 : Last 3 iteration, Mach: 0.6.

In the graphs presented presented in Figures 5.12, 5.13 and 5.14, the solutions for Mach numbers 0.3, 0.6, and 0.9. These graphs display the desired shape, the initial flight shape prior to optimization, and the flight shape resulting from the iterations. Notably, these graphs reveal that the aerodynamic lift coefficient of the flight shape

resulting from the optimization closely resembles that of the rigid shape. This similarity indicates that the optimization process successfully aligns the flight shape with the rigid shape in terms of aerodynamic performance. By iteratively refining the flight shape, the optimization procedure effectively minimizes the discrepancies between the initial and target shapes, demonstrating significant improvements in aerodynamic efficiency. This result highlights the effectiveness of the optimization method used, as it achieves an approximate version of the desired target shape, thereby improving the overall aerodynamic performance aircraft across various Mach numbers.

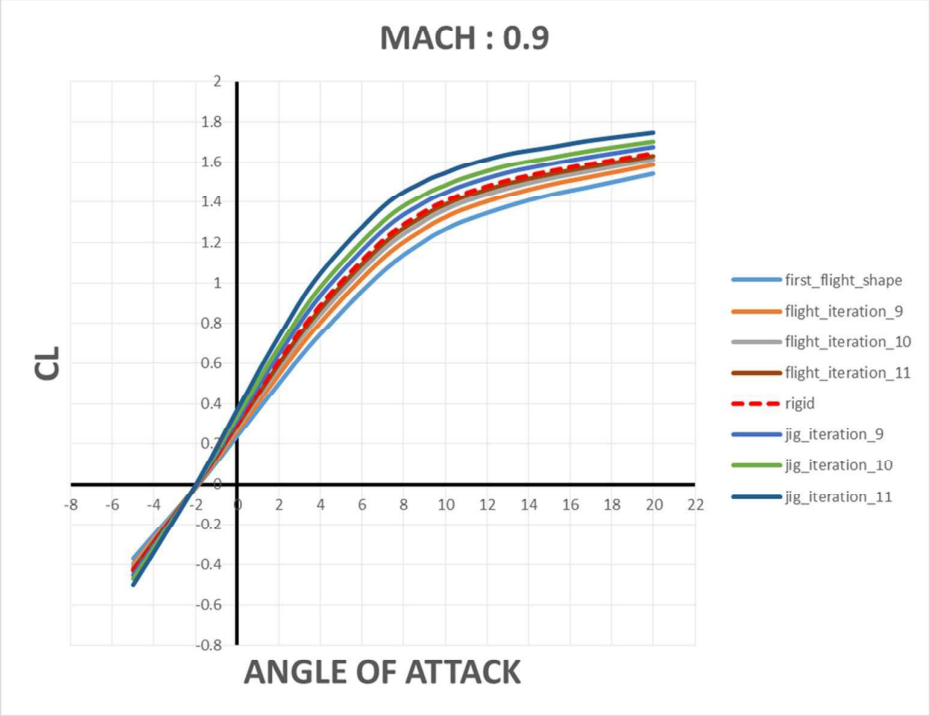

Figure 5.14 : Last 3 iteration, Mach: 0.9.

This achievement is particularly significant for high-altitude long-endurance (HALE) aircraft like the RQ-4 Global Hawk, where maintaining optimal aerodynamic performance is crucial for extended missions. The ability to closely match the desired aerodynamic shape ensures that the aircraft can perform efficiently, reducing drag and improving lift-to-drag ratios across different flight conditions. Moreover, the iterative optimization approach not only enhances the flight shape but also contributes to the structural integrity of the aircraft by ensuring that the aerodynamic loads are distributed more evenly. This leads to better performance and longevity of the aircraft. Overall, the results underscore the robustness and practicality of the optimization

method in real-world applications, demonstrating its potential to significantly enhance the operational capabilities of HALE UAVs.

Figure 5.15 shows the target shape, the initial flight shape, the jig shape after the last iteration, and the flight shape when flown with the final jig shape of the RQ-4 Global Hawk aircraft at Mach 0.3.

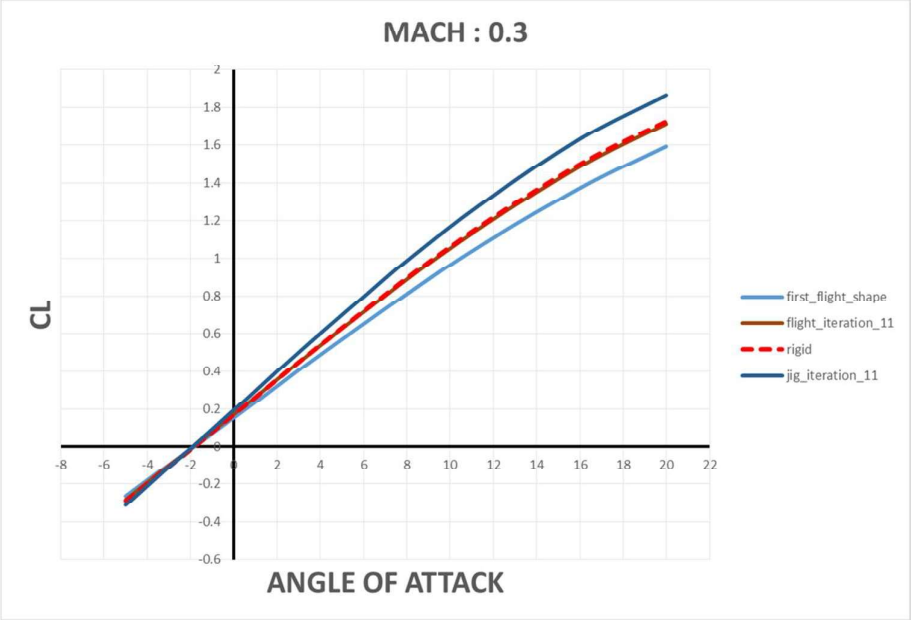

Figure 5.15 : First flight and last iteration result, Mach: 0.3.

Figure 5.16 shows the target shape, the initial flight shape, the jig shape after the last iteration, and the flight shape when flown with the final jig shape of the RQ-4 Global Hawk aircraft at Mach 0.6.

Looking at the results shown in Figures 5.15, 5.16, and 5.17, it is evident that with each iteration, the flight shape progressively approaches the desired shape. The graphs illustrate that the aircraft's design in the computer environment increasingly aligns with the target value. This highlights the importance of jig shape analysis. The method applied in this thesis will contribute to integrating jig shape analyses into the aircraft design process. When examining the results of our optimization model, it is evident that it operates very effectively. The graphs illustrate the model's performance across different Mach values, showing how the optimization adapts to varying flight conditions. The results shown in Figure 5.17 are particularly critical for this aircraft. As mentioned earlier, Mach 0.6 is within the operational range of this UAV.

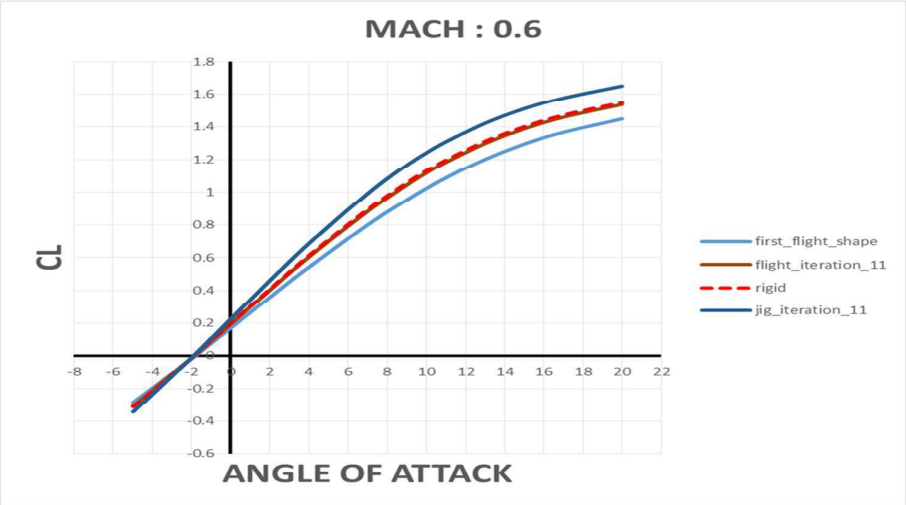

Figure 5.16 : First flight and last iteration result, Mach: 0.6.

Figure 5.17 shows the target shape, the initial flight shape, the jig shape after the last iteration, and the flight shape when flown with the final jig shape of the RQ-4 Global Hawk aircraft at Mach 0.9.

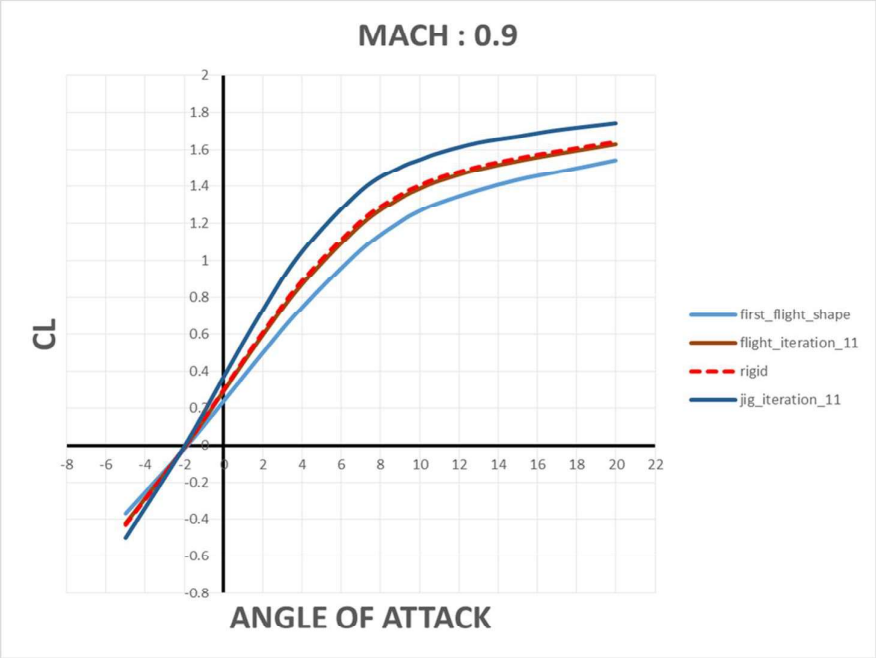

Figure 5.17 : First flight and last iteration result, Mach: 0.9.

Upon examining Figures 5.15, 5.16, and 5.17, the data in the lift coefficient - angle of attack graphs show that the optimization has been very successful.

6. CONCLUSION

The aim of this study is to optimize the jig shape of the RQ-4 Global Hawk aircraft to ensure that the produced aircraft flies with an aerodynamically optimized wing shape. Jig shape calculation is a long iterative process, and this study seeks to shorten and automate this lengthy iterative process. Existing studies in the literature have employed FSI methods, requiring expensive models and analyses that take hours or even days to calculate the jig shape for just one or a few points. In contrast, this study provides the capability to perform jig shape optimization at multiple points.

In this study, the cloud data of the RQ-4 Global Hawk aircraft found in the literature is used. Python scripts are employed to make this cloud data meaningful. These scripts separate the cloud data into components of the aircraft: the wing, fuselage, and vertical tail. The number of divisions for spanwise and chordwise sections is then fed as an input. The script collects the cloud points for the specified number of spanwise and chordwise sections. Connectivity is assigned to these points, making them interact with each other. Finally, all the components are assembled to ensure all nodes communicate. Since the ZONAIR solver performs better with structured mesh, the 3D structured mesh of the ZONAIR model is created using this procedure. Subsequently, the boundary conditions for the ZONAIR aerodynamic model are defined. The ZONAIR aerodynamic model is then solved for different Mach numbers and angles of attack. The aerodynamic data is then compared with the flight data of the RQ-4 Global Hawk aircraft shared in the literature, and the ZONAIR aerodynamic model is validated.

Similarly, the structural FEM model is created using the node and connectivity information from the ZONAIR aerodynamic model to form the structural mesh. The structural model then distributes the weight across the wing, fuselage, and tail to match the actual weight of the RQ-4 Global Hawk aircraft. The aircraft is modeled with composite materials, and density information. Each component is adjusted to achieve the correct weight. Since the RQ-4 Global Hawk is a military aircraft, its structural FEM model is not openly available in the literature. However, the stiffness data provided in the literature is used. The wing modes of the RQ-4 Global Hawk aircraft are identified and sent to the ZONAIR solver. In the aero-structural coupled model,

the aerodynamic and structural models interact with each other through spline coupling.

After setting up and validating the aerodynamic and structural models, the aero-structural model becomes ready. The ZONAIR model of the RQ-4 Global Hawk aircraft is tested, and the solution time is evaluated. The solution time for the structure-coupled model is less than one minute. This indicates that the elements in the model interact well with each other and that the model is robust. Otherwise, the solution time would be longer.

Under the defined flight conditions, the aero-structural coupled model performs rigid and elastic aerodynamic solutions using the ZONAIR solver. Subsequently, the difference caused by elastic effects between the elastic and rigid aircraft is calculated and illustrated in a graph. The RQ-4 Global Hawk aircraft has an aspect ratio of approximately 22.35, which is considerably high for aircraft. Due to this large aspect ratio, the RQ-4 Global Hawk is significantly affected by elastic effects. Therefore, optimizing the jig shape of the RQ-4 Global Hawk will enhance the aircraft's efficiency.

Jig shape optimization is a lengthy iterative process, and finding the correct shape is not easy. To determine the correct jig shape, optimization is necessary. When formulating the optimization problem, it is essential to accurately define the objective function, constraints, and design variables. In other words, the model for which you want to perform the jig shape optimization needs to be well-defined.

Examining the optimization results reveals that achieving the target shape during flight through jig shape optimization significantly enhances aircraft efficiency. Desired aerodynamic performance can be ensured during the design phase using jig shape optimization. A wing optimized solely for aerodynamics will not achieve the desired performance due to production constraints. Consideration of the target shape, flight shape, and jig shape during the aircraft design phase is crucial for improving the design. This study's approach to jig shape optimization focuses solely on aerodynamic optimization, allowing for jig shape adjustments without significantly altering the structural layout or increasing weight. The results from the present optimization showed that the optimal geometry can be achieved with far fewer elements, instead of optimizing approximately 50 million elements, highlighting the potential for

incorporating jig shape optimization into the preliminary design phase of the design cycle.

REFERENCES

[1] Jin, D., & Wang, Y. (2020). Research on Evolution Process and Control Method of External Shapes in the Life-cycle of Modern Civil Jets. IOP Conference Series: Materials Science and Engineering, 887(1), 012005

[2] Zhang, Y., Jia, D., Bontoft, E. K., & Toropov, V. (2022). Wing jig shape optimisation with gradient-assisted metamodel building in a trust-region optimisation framework. Journal Name, Volume(Issue), Sayfa Aralığı. doi: DOI numarası

[3] Huo, S. H., Wang, F. S., Yuan, Z., & Yue, Z. F. (2013). Mesh Regeneration Method for Jig-Shape Optimization: Design of the High-Aspect-Ratio Wing. *School of Mechanics Civil Engineering and Architecture, Northwestern Polytechnical University*, Xi'an 710129, China.

[4] Dowell, E. H. (2021). *Aeroelasticity of plates and shells*. Springer

[5] Hodges, D. H., & Pierce, G. A. (2011). *Introduction to structural dynamics and aeroelasticity*. Cambridge University Press

[6] Pak, C. (2021). *Jig-Shape Optimization of a Low-Boom Supersonic Aircraft*. NASA Armstrong Flight Research Center, Edwards, CA 93523-0273

[7] Jin, D., & Wang, Y. (2021). *Research on Evolution Process and Control Method of External Shapes in the Life-cycle of Modern Civil Jets*. Shanghai Aircraft Design and Research Institute, Shanghai, China

[8] Huo, S. H., Wang, F. S., Yuan, Z., & Yue, Z. F. (2013). *Mesh Regeneration Method for Jig-Shape Optimization Design of the High-Aspect-Ratio Wing*. School of Mechanics Civil Engineering and Architecture, Northwestern Polytechnical University, Xi'an 710129, China

[9] Bezuevsky, A. V., & Grigorev, A. V. (2021). *Rational Determination of Wing Jig Shape of a Long-Range Aircraft with Transonic Cruise Regime*. Central Aerohydrodynamic Institute (TsAGI), Zhukovsky, Russia

[10] Martins, J. R. R. A., Alonso, J. J., & Reuther, J. (2021). *Aero-Structural Wing Design Optimization Using High-Fidelity Sensitivity Analysis*. Department of Aeronautics and Astronautics, Stanford University, Stanford, CA 94305; NASA Ames Research Center, Moffet Field, CA 95035

[11] Sodja, J., Werter, N. P. M., & De Breuker, R. (2021). *Aeroelastic Demonstrator Wing Design for Maneuver Load Alleviation Under Cruise Shape Constraint*. Journal of Aircraft: devoted to aeronautical science and technology. DOI: 10.2514/1.C035955

[12] Moore, J. P. IV (2021). *Jig-Shape Optimization of a Flapping Wing for a Micro Air Vehicle*. Undergraduate, Aerospace Engineering, University of Florida

[13] Xiong, J., Nguyen, N., & Fugate, J. (2021). *Jig Twist Optimization of Mach 0.745 Transonic Truss-Braced Wing Aircraft and High-Fidelity CFD*

Validation. Stinger Ghaffarian Technologies, Inc., Moffett Field, CA 94035; NASA Ames Research Center, Moffett Field, CA 94035

[14] Martins, J. R. R. A., Alonso, J. J., & Reuther, J. (2021). *Aero-Structural Wing Design Optimization Using High-Fidelity Sensitivity Analysis*. Department of Aeronautics and Astronautics, Stanford University, Stanford, CA 94305; NASA Ames Research Center, Moffet Field, CA 95035

[15] Liu, X., Cheng, P., & Zhao, Y. (2021). *A Design Method for Twist Distribution along Wing Span*. Flight Physics Department, Shanghai Aircraft Design And Research Institute, COMAC, No.5188 Jinke Road, Pudong District, Shanghai, China

[16] Lyu, Z., Kenway, G. K. W., & Martins, J. R. R. A. (2014). *Aerodynamic Shape Optimization Investigations of the Common Research Model Wing Benchmark*. Published Online: 10 Oct 2014. DOI: https://doi.org/10.2514/1.J053318

[17] Allen, C. B., Poole, D. J., & Rendall, T. C. S. (2018). "Wing aerodynamic optimization using efficient mathematically-extracted modal design variables.". Published online: 1 March 2018. DOI: 10.1007/s10444-021-09870

[18] Hu, Z., Qiu, J., & Zhang, F. (2020). Fully Parametric Optimization Designs of Wing Components. *Beijing Key Laboratory of Civil Aircraft Structures and Composite Materials, Beijing Aeronautical Science & Technology Research Institute of COMAC, Beijing 102211, China*

[19] Elham, A., & van Tooren, M. J. L. (2016). Multi-fidelity wing aerostructural optimization using a trust region filter-SQP algorithm. Received: 10 May 2016; Revised: 16 October 2016; Accepted: 26 October 2016; Published online: 23 November 2016. This article is published with open access at Springerlink.com

[20] ZONA Technology.(2020). ZONAIR User's Manual Version 4.7. ZONA Technology

[21] Eaton, C. M., & Woolf, R. K. (2020). Flight Test Validation of the RQ-4 Block 20 Global Hawk Aerodynamic and Propulsive Models. U.S. Air Force Flight Test Center.

CURRICULUM VITAE

Name Surname **: Akın Ateş**

Place and Date of Birth **:**

E-Mail **:**

EDUCATION **:**

- B.Sc.2019, Istanbul Technical University, Faculty of Aeronautics and Astronautics, Astronautical Engineering Departm